Provenance of the Cretaceous–Eocene Rajang Group submarine fan, Sarawak, Malaysia from light and heavy mineral assemblages and U-Pb zircon geochronology

Thomson Galin [a,b], H. Tim Breitfeld [a], Robert Hall [a], Inga Sevastjanova [a,c]

[a] *SE Asia Research Group, Department of Earth Sciences, Royal Holloway University of London, Egham, TW20 0EX, UK*

[b] *Minerals and Geoscience Department Malaysia (JMG) Sarawak, Jalan Wan Abdul Rahman, Kenyalang Park P.O. Box 560 93712 Kuching, Sarawak, Malaysia*

[c] *Getech Group plc, UK, Leeds, LS8 2LJ, UK*

Keywords: Provenance, Zircon U-Pb ages, Rajang Group, Sarawak, SE Asia

Abstract

The Rajang Group sediments in central Borneo form a very thick deep-water sequence which was deposited in one of the world's largest ancient submarine fans. In Sarawak, the Lupar and Belaga Formations form the Rajang Group, characterised by turbidites and large debris flows, deposited in an interval of at least 30 Ma between the Late Cretaceous (Maastrichtian) and late Middle Eocene. Borneo is one of the few places in SE Asia where sediments of this age are preserved. Heavy mineral assemblages and detrital zircon U-Pb dating permit the Rajang Group to be divided into three units. The Schwaner Mountains area in SW Borneo, and West Borneo and the Malay Tin Belt were the main source regions and the contribution from these source areas varied with time. Unit 1, of Late Cretaceous to Early Eocene age, is characterised by zircon-tourmaline-dominated heavy mineral assemblages derived from both source areas. Unit 2, of Early to Middle Eocene age, has zircon-dominated heavy mineral assemblages, abundant Cretaceous zircons and few Precambrian zircons derived primarily from the Schwaner Mountains. Unit 3, of Middle Eocene age, has zircon-tourmaline-dominated heavy mineral assemblages derived from both sources and reworked sedimentary rocks. There was limited contemporaneous magmatism during deposition of the Rajang Group inconsistent with a subduction arc setting. We suggest the Rajang Group was deposited north of the shelf edge formed by the Lupar Line which was a significant strike-slip fault.

1. Introduction

The central part of Borneo is a long arcuate mountain belt that forms the border between Sarawak and Kalimantan and southern Sabah. It includes a very thick clastic sedimentary succession named the Belaga Formation (Liechti et al., 1960) in Malaysia with equivalents in Kalimantan (Pieters et al., 1987) assigned to the Rajang Group (Hutchison, 1996) (Fig. 1). This extends offshore beneath the hydrocarbon-bearing basins of Sarawak (e.g. Madon, 1999; Mat-Zin, 2000).

Van Bemmelen (1949) and Milroy (1953) were the first to describe the sedimentary succession in central Borneo, and were followed by memoirs and reports from geological survey geologists (Haile, 1957; Kirk, 1957; Wolfenden, 1960; Tan, 1979). These descriptions were summarised for Central Sarawak by Liechti et al. (1960). Haile (1974) introduced the term Sibu Zone for the part of Sarawak north of the Lupar Line composed predominantly of the Belaga Formation, which forms the major part of the Rajang Group in Sarawak. The Sibu Zone (Central Sarawak) forms an approximately 200 km wide zone north of the Lupar Valley and south of the Bukit Mersing Line (Fig. 1). It comprises highly deformed, steeply dipping sedimentary and low-grade metasedimentary rocks. Haile (1968) introduced geosynclinal terminology to NW Borneo and interpreted the Rajang Group as flysch deposits in a eugeosynclinal furrow. Later, the Rajang Group sediments were recognised as deep marine turbiditic rocks (Tan, 1979; Hutchison, 1996, 2005; Bakar et al., 2007). With the emergence of plate tectonics, a role for subduction and collision was inferred and the Rajang Group was assumed to be related to an accretionary setting (e.g. Hamilton, 1979; Tan, 1979; Hutchison, 1996) although Moss (1998) questioned this interpretation. Hutchison (2010) described the central Borneo mountain belt as an orocline.

The extent, thickness, structure and tectonic setting of the Rajang Group remain uncertain and its age is based on limited foraminifera data (Kirk, 1957; Liechti et al., 1960; Wolfenden, 1960; Tan, 1979). Various suggestions have been made for the source of the clastic sediments. They include a southern (Tan, 1982) and potentially a northern (Pieters and Sanyoto, 1993; Pieters et al., 1993) source, Indochina (Hamilton, 1979), proto-Mekong River (Hutchison, 1989), Thailand, Indochina and Malay Peninsula (Moss, 1998), Sunda Shield (Hazebroek & Tan, 1993) and the Schwaner Mountains of Kalimantan (Williams et al., 1988). There have been no provenance studies that can be used to assess these suggestions.

This study presents new results based on field investigations, petrography, light and heavy mineral analyses, and U-Pb dating of detrital zircons. It reconstructs the provenance of the Rajang Group and discusses the tectonic setting of deposition.

2. Geological background

2.1. Rajang Group

The Belaga Formation and the Lupar Formation form the Rajang Group in Central Sarawak. The Lupar Formation has been considered to underlie the Belaga Formation but is exposed only in a narrow fault-bounded ridge at the northern margin of the Lupar Valley (Haile, 1957; Tan, 1979). It differs slightly from the Belaga Formation in having overall a more arenaceous character than the lower parts of the Belaga Formation (Liechti et al., 1960), some interbedded basic rocks (Haile et al., 1994) and the occurrence of some boudinaged blocks (Tan, 1979). Both formations are discussed in detail below. Other formations that have been assigned to the Rajang Group include the Kelalan Formation and the Mulu Formation in North Sarawak, the Embaluh Group of Kalimantan, and the Sapulut Formation in Sabah (Haile, 1962; Collenette, 1965; Tate, 1991; Hutchison, 1996; Moss, 1998). In NE Kalimantan the Lurah, Mentarang and Long Bawan Formations may be equivalents of the deep marine Belaga Formation (B.R.G.M, 1982) and were interpreted as continuation of the Rajang Group (Pieters et al., 1987; Hutchison, 2010). Here we are concerned only with the Belaga Formation and the Lupar Formation.

The Rajang Group is described by Hutchison (1996) as "a monotonous flysch group of interbedded sandstone and mudstone locally metamorphosed to lower greenschist facies phyllite and slate". Haile (1974) suggested a thickness of 15 km although Hutchison (1996) commented that the basis for this estimate is unknown. Hutchison (2005) estimated 4.5 to 7.5 km for the Belaga Formation and Tan (1979) estimated 500 m for the Lupar Formation. It is not certain what lies underneath the Belaga Formation. Moss (1998) assumed ophiolitic basement, Hutchison (2010) inferred oceanic crust, and Breitfeld et al. (2017) suggested a composite basement including some accreted continental crust. Within the upper parts of the Rajang Group are some magmatic rocks interpreted as Eocene (Kirk, 1957). These include Bukit Mersing basic rocks and acid magmatic rocks in the Arip-Pelungau valley.

The formation is highly deformed. Hutchison (1996, 2005) referred to the Rajang Group sediments as an Eocene accretionary complex and attributed deformation and uplift to a Late Eocene Sarawak Orogeny caused by collision of a continental promontory of the Miri Zone-Central Luconia Province of northern Sundaland. However, Wolfenden (1960) had noted the absence of a marked angular unconformity in some areas and commented that the "stratigraphic evidence is difficult to reconcile with the concept of an Upper Eocene orogeny that caused the entire… …Rajang Group to be folded" and that "deformation accompanied deposition". In contrast, Moss (1998) interpreted the sediments to represent parts of a remnant ocean basin. Hall (2012) and Hall and Sevastjanova (2012)

supported this interpretation and questioned the interpretation of deformation as the result of a collisional Sarawak Orogeny. Instead they suggested there was deep-water syn-depositional deformation between the Late Cretaceous and the Late Eocene, as originally proposed by Wolfenden (1960). The major unconformity that terminates Rajang Group sedimentation and the change to little deformed shallow and marginal marine sediments was suggested to mark a regional plate reorganisation that occurred when Australia began to move north at about 45 Ma, initiating subduction beneath Sabah of the proto-South China Sea and renewed subduction south of Java (e.g. Hall, 2002, 2012; Hall et al., 2008, 2009). Hall and Breitfeld (2017) termed this the Rajang Unconformity (Fig. 2).

2.2. Post-Rajang Group in Sarawak

Hutchison (1975) presumed the upper contact of the Belaga Formation to be a fault zone characterised by ophiolite and related rocks and named it the Bukit Mersing Line, although he later doubted this interpretation (Hutchison, 2005). This is the boundary between Central and North Sarawak (Liechti et al., 1960) and between the Sibu and Miri Zones (Haile, 1974). The Belaga Formation is unconformably overlain by Paleogene to Neogene sediments in the Miri Zone. These include the Tatau and the Nyalau Formations (Kirk, 1957; Liechti et al., 1960), sediments of the Mukah-Balingian province (Wolfenden, 1960; de Silva, 1986) and the ambiguous Tunggal-Rangsi conglomerate (Liechti et al., 1960; Mat-Zin, 2000). Some inliers of Nyalau Formation are reported from the Sibu Zone (Kirk, 1957).

There was Plio-Pleistocene volcanism (Kirk, 1957; Cullen et al., 2013) in the Sibu Zone in the upper Rajang River and adjacent areas (Fig. 1 and 2) including the Usun Apau and Linau-Balui Plateaux, the Hose Mountains and the Nieuwenhuis Mountains.

3. Stratigraphy of the Rajang Group in Sarawak

3.1. Lupar Formation

The Lupar Formation includes the oldest rocks of the Rajang Group. It contains foraminifera in shales indicating an age not older than Cenomanian, with Turonian to Maastrichtian foraminifera in coarser samples (W.E. Crews in Milroy, 1953). Tan (1979) considered some of these samples to represent the Lubok Antu Melange and parts to be Lupar Formation and reported foraminifera of probable Santonian to Maastrichtian age. Tan (1979) concluded the Lupar Formation rocks were turbiditic deposits from graded bedding, sole marks and rhythmically interbedded shales and sandstones.

The base of the formation is not exposed, but is assumed to be in fault contact with the Lubok Antu Melange. The northern top of the formation was considered a transition into the Layar Member of

the Belaga Formation by Liechti et al. (1960) or in parts a fault contact by Tan (1979). The formation is intruded by and interbedded with rocks of the Pakong Mafic Complex (Tan, 1979; Haile et al., 1994).

3.2. Belaga Formation

The Belaga Formation has been described as a low grade metamorphic shale succession with intercalations of greywacke and sub-greywacke sandstone (Liechti et al., 1960). It is now considered to be largely turbidite sequences that were deposited in a deep marine environment (e.g. Tan, 1979, 1982; Tongkul, 1997; Honza et al., 2000; Hutchison, 2005; Bakar et al., 2007). Thick bedded sandstones in the Pelagus, Metah and Bawang Members were interpreted as debrites by Bakar et al. (2007).

Four subdivisions of the Belaga Formation called stages were recognised by Crews and John (in Milroy, 1953) in Central Sarawak with proposed ages based on paleontological evidence: Turonian to Maastrichtian Stage I, Paleocene to Early Eocene Stage II, Middle to Late Eocene Stage III and Late Eocene Stage IV. The ages were later supplemented by data from Haile (1957), Kirk (1957) and Wolfenden (1960). The stages were the basis for mapping of the Belaga Formation by Haile (1957) in the Lupar and Saribas valleys, Kirk (1957) in the Upper Rajang area, and Wolfenden (1960) in the Lower Rajang area. Attempts were made to map the Belaga Formation based on lithology and the Belaga Formation was later divided into members (Liechti et al., 1960) and each was assigned a type section or type area. Liechti et al. (1960) observed that “it has to be admitted that they are not pure rock-stratigraphic units. Not only has paleontological distinction preceded their creation, but their identification on lithology is only approximately possible”. The members (Fig. 2) from south to north (i.e. oldest to youngest) are: Upper Cretaceous (Turonian-Maastrichtian) Layar Member (previously Stage I), Paleocene to Lower Eocene Kapit Member (previously Stage II), Middle Eocene to Upper Eocene Pelagus Member (previously Stage III), Upper Eocene Metah Member (previously Stage IV) and Bawang Member of suggested Eocene age which occurs within the Miri Zone (previously Bawang Formation). Hutchison (2005) suggested the Layar Member was Cenomanian-Turonian, the Pelagus Member to be Early to Middle Eocene and the Metah Member to be Middle to Late Eocene.

4. Sampling and methodology

For this study fieldwork was carried out in the Sibu Zone. In the western part of the study area sampling was undertaken mainly along the Pan-Borneo Highway from the Lupar valley to Tatau and on minor roads and small logging tracks in the interior. The upper reaches of the Rajang River from the town of Kapit to the Pelagus and Mikai Rapids were traversed by boat.

4.1. Sampling

Sandstones and siltstones from the Lupar Formation and all members of the Belaga Formation were sampled for light and heavy mineral analysis, and zircon dating. The geological map of the Sibu Zone (Fig. 2) shows the location of samples.

Detrital modes for light minerals were determined using the Gazzi-Dickinson method (Gazzi, 1966; Dickinson, 1970; Gazzi et al., 1973) and the Glagolev-Cheyes method (Galehouse, 1971) on stained thin sections. Sodium cobaltinitrite was used for staining alkali feldspar and barium chloride and amaranth solution was used for staining plagioclase.

4.2. Sample preparation for mineral analysis

Sample preparation for heavy mineral analyses was carried out at Royal Holloway University of London. The samples were crushed and a 63-250 µm fraction was separated by sieving. Heavy minerals from this fraction were separated using standard heavy liquid Lithium heteropolytungstate (LST) at a density of 2.89 g/cm³. The heavy mineral separates were further processed by a FRANTZ magnetic barrier separator and by standard heavy liquid Di-iodomethane (DIM) at 3.3 g/cm³ to concentrate zircons. Zircon grains between 63 and 250 µm were hand-picked or poured and mounted in epoxy resin blocks and polished to expose mid-grain sections. The mounted zircons were imaged in transmitted light and with cathodoluminescence secondary electron microscope (CL-SEM) to select analysis spots for each grain and to detect cracks and inclusions, and zoning of zircons prior to the LA-ICP-MS age analysis.

4.3. LA-ICP-MS U-Pb geochronology

LA-ICP-MS (laser ablation inductively coupled plasma mass spectrometry) dating of zircons from 12 samples was carried out at Birkbeck College, University of London. Zircon U-Pb dating was performed on a New Wave NWR 193 and NWR213 nm laser ablation system coupled to an Agilent 7700 quadrupole-based plasma mass spectrometer (ICP–MS) with a two-cell sample chamber. A spot size of 25 µm for the NWR 193 nm and of 30 µm for the NWR 213 nm system was used. The Plešovice zircon standard (337.13 ± 0.37 Ma; Sláma et al., 2008) and a NIST 612 silicate glass bead (Pearce et al., 1997) were used to correct for instrumental mass bias and depth-dependent inter-element fractionation of Pb, Th and U.

GLITTER data reduction software (Griffin et al., 2008) and the common lead correction method by Andersen (2002), which is used as a ^{204}Pb common lead-independent procedure, were used. The age obtained from the ^{207}Pb/^{206}Pb ratio is given for grains older 1000 Ma. Because ^{207}Pb cannot be measured with sufficient precision in grains which are younger than 1000 Ma and thus results in

large analytical errors (Nemchin and Cawood, 2005), the age obtained from the $^{238}U/^{206}Pb$ ratio is given. Concordance was tested by using a 10% threshold. For ages greater than 1000 Ma the $^{207}Pb/^{206}Pb$ and $^{206}Pb/^{238}U$ ages were used to assess concordance, and for ages below 1000 Ma the $^{207}Pb/^{235}U$ and $^{206}Pb/^{238}U$ ages. Age histograms and probability density plots were created using an R script that adepts the approach of Sircombe (2004) for calculating probability density. All analyses data are compiled in the Supplementary Tables 1 to 12.

5. Field observations

5.1. Lupar Formation

The Lupar Formation is composed of sandstone beds rhythmically interbedded with shale, siltstone and mudstone (Fig. 3A). The sandstone beds are generally graded, and slumping (Fig. 3B) is common. Sandstone beds are rarely thicker than a few centimetres and usually scour into the mud/shale layers. The sedimentological characteristics indicate deposition as a turbidite with common occurrence of Bouma A and B units. The sedimentological and lithological features of the Lupar Formation are very similar to the overlying Layar Member of the Belaga Formation except for an overall more arenaceous character (Liechti et al., 1960).

5.2. Layar Member

The Layar Member is a moderate to steeply dipping (44-71°) folded succession of metamorphosed shales, siltstones and sandstones (Fig. 3C). The predominant lithology is metamorphosed shales that occur as thick beds or alternations with thin siltstones or sandstones. Typical successions within the Layar Member include: 1) thick beds (up to a few metres) of shale. The shale is generally grey to dark grey and is variably metamorphosed into slate and phyllites. 2) Shale and siltstones interbedded with sandstones of uniform thickness between a few centimetres to a few tens of centimetres. 3) Thicker sandstones from tens of centimetres to a metre in thickness (Fig 3E). The sandstones are massive, and typically have scoured bases. 4) Conglomerate beds usually composed of syn-sedimentary deformed shale clasts within a matrix of fine to coarse sand (Fig. 3E and F). The beds usually have erosive bases and flat tops.

The sandstones of the Layar Member generally vary from fine to coarse grained, and the thinner beds are usually of finer grain size. Slumping is quite common within the successions with chaotically deformed beds found between undisturbed beds (Fig. 3D). The undisturbed sandstones occur as beds showing ripples, parallel laminations or normal grading (Fig. 3G and H). Thick beds occur sporadically and are commonly cut by quartz veins. The sandstones towards the Sarawak interior in the east are generally much thicker bedded than in the west. There are also some locations in the interior that expose slates to low-grade schists (Fig. 3I).

The Layar Member is interpreted as distal turbidites based on the predominance of shale interbedded with thin sandstone and siltstone beds, and the usually thin character of the sandstones. Bouma units D and E are dominant. The sandstones represent episodes of turbidite (Bouma A and B) input that scour into the shale beds. Occasionally, there were debris flows represented by conglomerate beds containing shale clasts eroded from the earlier deposited shales (mudflake conglomerates). Slumping is quite common and is represented by chaotically deformed beds.

5.3. Kapit Member

The Kapit Member is composed of metamorphosed shale interbedded with sandstone and siltstone with dips of 60° to 90°. Overturned sections were also observed. Typical successions are composed of: 1) thick shales that are variably metamorphosed to slate (a few metres thick). 2) Shales interbedded with siltstones and sandstones which are a few centimetres to tens of centimetres in thickness. 3) Thickly bedded sandstones (up to two metres).

Sandstones up to 60 centimetres thickness were deposited sporadically within the succession (Fig. 4A and B). Load structures are usually present at the base of the sandstone beds. In the Bukit Sebangkoi area, representing stratigraphically the lower part, the Kapit Member is dominated by sandstone. Towards Sibu, the middle part of the Kapit Member becomes progressively dominated by grey shale and siltstones and sandstones a few centimetres to tens of centimetres thick. Some thick beds of sandstone do occur and are sometimes composed of sub-rounded and elongate clasts of finer grained material within a coarse sandstone matrix. Large scale slumping is also seen within the succession (Fig. 4C).

In the interior in the Rajang River and near Sibu, where the stratigraphically higher part of the Kapit Member is exposed, a typical succession is represented by alternation of thin sandstones and shales or siltstones (2 cm-10 cm) passing up into thicker beds (a few tens of centimetres) followed by thickly interbedded, often amalgamated, sandstones. The fresh sandstone in the Upper Rajang area is grey in colour and is very hard. The thinner sandstones are usually finer grained and the thicker sandstone is usually coarser grained. Load structures are quite common on the lower bed surfaces of the sandstones (Fig. 4D) and the bases are erosive. Upright tight folding was observed (Fig. 4E).

The Kapit Member samples are turbidites. The lower part of the Kapit Member is similar to the underlying Layar Member whereas the upper part resembles the overlying Pelagus Member.

5.4. Pelagus Member

The Pelagus Member is the most arenaceous member of the Belaga Formation. The predominance of sandstone beds is the main characteristic of the Pelagus Member. Typical successions within the Pelagus Member include: 1) interbedded thin (5-10 cm) shale and siltstone or sandstone. 2) Interbedded sandstones of variable thickness (10 cm-2 metres) with minor shale.

South of Sibu, the lower part of the Pelagus Member is composed of interbedded shale and siltstone and sandstone overlain by thick sandstones with erosive bases (Fig. 5A and B). Slumping was observed (Fig. 5C). Generally two types of sandstones can be identified. The first is grey coloured and poorly sorted sandstone, with turbiditic character. The other is the lighter coloured and is usually thickly bedded (60 cm to 1 metre) amalgamated sandstone interpreted as a debris flow deposit. The sandstones in the Pelagus Member show rippled surfaces (Fig. 5D), minor bioturbation (Fig. 5E) and parallel lamination (Fig. 5F). Load structures are commonly found at the base of thicker sandstone beds (Fig. 5G). In the interior (Rajang River, Bukit Tanggi quarry), the Pelagus Member consists of thickly bedded sandstones interbedded with minor shales (Fig. 5H) cut by thin calcite veins.

Convolute bedding (Fig. 6A) and polygonal faulting resulting from soft-sediment deformation was observed (Fig. 6B). Beds containing mud clasts similar to the lower members are also found within the succession (Fig. 6C). Displacement of mud-silt-sandstone alternations (heterolithics) in thick amalgamated sandstone packages (Fig. 6D) is also attributed to soft-sediment deformation. The shale is grey in colour and shows cleavage, while sandstones have often a reddish-pinkish colour.

The Pelagus Member represents proximal turbidites with abundant Bouma A and B units. The Pelagus Member is dominated throughout the succession by thick amalgamated sandstone beds that represent debrites.

5.5. Metah Member

The Metah Member consists of interbedded shale, siltstones and sandstones. In contrast to the Pelagus Member the abundance of thick sandstone beds decreases and shale and mudstone dominate. The Metah Member is tightly folded and dips steeply to the south and north (Fig. 6E). The member is almost unmetamorphosed or metamorphosed at a lower grade compared to the other members of the Belaga Formation.

Typical successions are composed of: 1) Thick beds of grey shale (a few metres thick) (Fig. 6F), 2) interbedded shales and siltstones with variable thickness. The shale is commonly interbedded with thin (2-3 cm) layers of siltstones and sandstones. The sandstones are variable in thickness (20-40 cm)

and generally show variable thickening and thinning across the succession and 3) thickly interbedded sandstones (up to 2 metres) with minor shale.

The thicker beds are usually coarse grained lighter coloured amalgamated sandstones with scoured bases (Fig. 6G). Occasionally clast-supported conglomerates, consisting of clasts of mudstone within a matrix of sand, were also deposited (mudflake conglomerates). In the Upper Rajang River area, the Metah Member is represented by fine to medium grained sandstone (up to 30 cm thick) interbedded with 15 cm thick shales.

The Metah Member represents return to a quieter environment with deposition of distal turbidites with Bouma C, D and E units, similar to those of the Layar and lower Kapit Members of the Belaga Formation. However, thick amalgamated sandstone beds indicate deposition of debrites between intervals of distal turbidites.

5.6. Bawang Member

The Bawang Member is exposed in deeply weathered sections in the Tatau area, separated from other Rajang Group members. The top appears to be an unconformity and is overlain by the Tunggal-Rangsi Conglomerate (Fig. 6I). The Bawang Member consists predominantly of shale that is commonly interbedded with siltstones and sandstones (Fig. 6H). Calcareous shales were also observed. The sandstones contain laminations of dark coloured mudstone. However, thicker (up to 30 cm) sandstones were also observed that are interpreted as amalgamated beds. The shales of the Bawang Member are usually metamorphosed and bedding is cut by cleavage. The sandstones have commonly scoured bases, indicating erosion into the underlying beds.

The predominance of shale shows the Bawang Member represents a quiet environment with deposition of distal turbidites; amalgamated sandstone beds indicate input of debrites between quieter intervals.

6. Petrography

6.1. Light mineral detrital modes

Light mineral compositions for all samples are displayed in Table 1. Most samples are quartz-dominated with abundant lithic fragments of various origins and both feldspar varieties. Samples with matrix proportions of 0-15% are mainly classed as sublitharenite or subarkose in the QFL diagram of Pettijohn et al. (1987) and samples with 15-75% as lithic or feldspathic greywacke (Fig. 7). Samples from the Lupar Formation and Layar Member are predominantly lithic greywackes or sublitharenites characterised by high matrix content and an abundance of lithic fragments. Samples from the lower Kapit Member are sublitharenites to subarkoses with abundant lithic fragments. In

contrast, the Pelagus and upper Kapit Member samples are predominantly subarkoses with feldspar more abundant than lithic fragments and low proportions of matrix. The Metah Member samples are sublitharenites or lithic arenites characterised by low proportions of matrix similar to the Pelagus Member, but with lithic fragments more abundant than feldspar. The two samples from the Bawang Member are a lithic arkose and feldspathic greywacke and are the most feldspathic of the data set.

Provenance from the light mineral assemblage is displayed on the QFL and QmFLt diagrams of Dickinson et al. (1983). The samples cluster in the recycled orogenic field in the QFL diagram (Fig. 7). Provenance of the samples in the QmFLt diagram cluster around the mixed field, with some samples fall into the dissected arc and transitional recycled field (Fig. 7). Polycrystalline quartz and metamorphic lithic fragments indicate a metamorphic source. Volcanic quartz and lithic fragments show input of volcanic material. Sedimentary lithic fragments reveal recycling of previous sedimentary cover including cherts which may be deep marine or diagenetic.

6.2. Textures

Sandstones from the Rajang Group generally contain sub-angular to sub-rounded grains with a few angular and rounded grains. Their high quartz contents and the low abundance of feldspars and lithic grains indicates compositional maturity but the angular to sub-angular grain shape observed in many samples implies textural immaturity. The apparent compositional maturity may partly reflect breakdown of unstable grains (Cummins, 1962) or diagenesis (Williams et al., 1954; Allen, 1964), both likely in a tropical setting (Sevastjanova et al., 2012).

6.3. Heavy minerals

Heavy minerals from the Lupar and Belaga Formation are shown in transmitted light (Fig. 8) and backscattered SEM (Fig. 9A and B) images. Heavy mineral counts are listed in Table 2.1 and percentages are in Table 2.2.

6.3.1. Lupar Formation

One sample of the Lupar Formation (TB39) was analysed (Fig. 10A). It is dominated (80.5%) by ultra-stable zircon which includes colourless and pink varieties with predominantly subhedral to subrounded grain shapes. The remaining 19.5% of heavy minerals include rutile, brookite, anatase, garnet, titanite, tourmaline, epidote, chrome spinel, pyroxene and chlorite.

6.3.2. Layar Member

Samples TB40 and TB179b were analysed from the Layar Member. TB179b is dominated by tourmaline (74.2%), zircon (24.2%) and rutile (1.3%). TB40 also contains tourmaline (47.2%), zircon

(45.2%) and rutile (2.6%), but also garnet (3.0%), chlorite (1.0%) and chrome spinel (0.7%). In both samples traces of epidote (0.3%) were observed. Tourmaline is predominantly brown in both samples. Zircon is mostly colourless euhedral, subhedral and anhedral grains. Both samples contain purple zircon. The Layar Member is dominated by tourmaline and zircon (Fig. 10A) with small amounts of rutile, in marked contrast to the zircon-dominated Lupar Formation.

6.3.3. Kapit Member

Samples TB189a, TB43 (both from the western road section) and TB238 (interior Rajang River section) were analysed from the Kapit Member (Fig. 10A). There is a marked change from a tourmaline-zircon-dominated assemblage in the south (lower Kapit Member) to a zircon-dominated assemblage in the upper Kapit Member. TB189a is from the lower part of the Kapit Member and resembles the Layar Member with tourmaline (57.0%), zircon (41.0%) and rutile (2.0%). TB43 and TB238 are from the upper part of the Kapit Member and both are dominated by zircon. TB43b contains zircon (77.4%), tourmaline (8.2%), chlorite (7.2%), garnet (3.9%), chrome spinel (1.3%), apatite (1.0%), rutile (0.7%) and epidote (0.3%). TB238 has zircon (73.9%), tourmaline (17.3%), rutile (4.9%), garnet (1.3%), apatite (2.3%) and epidote (0.3%). In all Kapit Member samples tourmaline is mostly brown. Morphologies of zircon are diverse and include colourless euhedral, anhedral, subrounded, and rounded types. Purple zircons are present in all three samples.

6.3.4. Pelagus Member

Pelagus Member samples TB44 and TB197a were sampled from the western road section and TB241 was sampled in the interior (Fig. 10A). TB44 is the oldest sample from the Pelagus Member and contains zircon (71.1%), garnet (13.2%), tourmaline (11.5%), rutile (3.0%), epidote (0.7%) and traces (0.3%) of chrome spinel and monazite. TB197a contains only zircon (79.1%), tourmaline (17.3%) and rutile (3.6%). The inland sample, TB241, contains zircon (78.7%), tourmaline (9.3%), apatite (7.3%), garnet (2.7%), rutile (0.7%) and epidote (0.3%). Tourmaline is predominantly brown and is the Mg end-member dravite. Zircons are diverse, including colourless and some purple euhedral, anhedral and subhedral, and subrounded to rounded types.

6.3.5. Metah Member

Samples TB195 and TB203a were collected close to each other from the Metah Member along the western road section (Fig. 10A). TB195 is stratigraphically higher than TB203a. TB195 contains zircon (60.0%), tourmaline (38.0%), rutile (1.7%) and garnet (0.3%). TB203a is almost identical and contains zircon (57.3%), tourmaline (37.0%) and rutile (4.7%). Tourmaline is predominantly a brown variety,

similar to other members. Zircon types are diverse, but most commonly are colourless subrounded, colourless anhedral and colourless rounded.

6.3.6. Bawang Member

Two samples were analysed from the Bawang Member and both are dominated by zircon. TB47, from the lower part of the Bawang Member (Fig. 10A), contains zircon (77.9%), tourmaline (15.5%), rutile (0.6%), garnet (5.7%) and epidote (0.3%). Higher in the Bawang Member rutile becomes more abundant and TB199a is composed of zircon (71.0%), tourmaline (17.0%), rutile (6.3%), garnet (4.3%) and chlorite (1.3%). The Bawang Member is dominated by euhedral to subhedral zircon.

6.4. Heavy mineral ratios

The commonly used indices of Morton and Hallsworth (1994) were not used for the samples analysed, because of the low abundance or absence of most heavy minerals except the ultra-stable minerals. The zircon-tourmaline index (ZTR) of Hubert (1962) and the zircon-tourmaline ratio (ZTi) (e.g. Mange and Wright, 2007) are more useful (Fig. 10B). The ZTR index is interpreted to indicate composition and maturity of the heavy mineral assemblage, while the ZTi ratio reflects transportation due to the density differences of the two minerals (e.g. Mange and Wright, 2007). The abundance of Ti minerals varies but identifying them consistently can be difficult and their abundance can be affected by authigenic growth of brookite and anatase as well as secondary rutile needle growth. All heavy mineral indices are displayed in Table 3.

ZTR of all samples is very high, ranging from 85 to 100, indicating the maturity of the heavy mineral assemblage (Fig. 10B). ZTi shows some very interesting variations through the succession (Fig. 10B). The ZTi of the Lupar Formation is 93.6 but drops significantly to 24.6-48.93 in the Layar Member. The lower Kapit Member has a similar ZTi of 41.8. The upper Kapit Member and the overlying Pelagus Member samples have high ZTi values above 80. The Metah Member samples have a significantly lower ZTi of c. 61. The Bawang Member samples have ZTi values of about 80 similar to the upper Kapit and Pelagus Members. These variations could be related to source differences. Alternatively, low ZTi values for the Layar Member, lower Kapit Member and the Metah Member could reflect hydraulic sorting, potentially related to a long transport distance and/or high energy environment, whereas the higher ZTi values could be a result of shorter transport distance or lower energy environments.

6.5. Zircon varietal studies

The zircons in the Lupar and Belaga Formations are colourless, purple, brown and yellow. Colourless zircons are most abundant, followed by purple, brown and yellow zircons. Fig. 9B displays

backscattered SEM images of zircon varieties observed in the Rajang Group. All types occur as rounded and non-rounded grains indicating a mixture of less and greater recycled material. Euhedral zircons are less than 10% of the total and elongate zircons are present in small numbers. The euhedral and elongate zircons represent first/few cycle zircons. Tab. 2 displays percentage of angular to rounded zircon varieties. Samples from the Lupar Formation and the Layar Member have abundant rounded zircons (41.1 to 51.6%). The lower Kapit Member sample is dominated by angular zircons (68.3%). Samples from the upper Kapit and Pelagus Member have predominantly angular zircons (54.5 to 79.7%), while samples from the Metah Member show a significant amount of rounded zircons (45.6 to 53.5%). Angular zircons dominate again in samples from the Bawang Member (70.4%).

7. U-Pb Geochronology

7.1. Lupar Formation

114 concordant U-Pb ages were obtained from 130 zircon grains (Fig. 11) in a lithic greywacke sample (TB39). There are 95 Phanerozoic and 19 Proterozoic ages ranging from 70 ± 1 Ma (Maastrichtian, Late Cretaceous) to 2457 ± 22 Ma (Paleoproterozoic). The major age populations are Cretaceous, Permo-Triassic and around 1.8 Ga. The Cretaceous population is the largest and has a major peak between 110 and 130 Ma. The Permian-Triassic population ranges from around 210 to 270 Ma with a major peak between 240 to 260 Ma. There are a small number of Jurassic and Carboniferous to Ordovician ages. The major Proterozoic peak at 1.8 Ga is accompanied by a few grains with ages at around 800 to 900 Ma, at 2.1 Ga and at 2.4 Ga. The Mesozoic and Paleozoic zircons are dominated by subrounded grains indicating moderate recycling with subordinate euhedral and rounded zircons. Proterozoic zircons are mainly rounded and are interpreted as the product of multiple recycling.

7.2. Belaga Formation

7.2.1. Layar Member

126 concordant U-Pb ages were obtained from 135 zircon grains of sample TB40 from the lower part of the Layar Member (Fig. 11). This sample is similar to TB39 of the Lupar Formation. There are 92 Phanerozoic, 31 Proterozoic and 3 Archean ages from 76 ± 1 Ma (Campanian, Late Cretaceous) to 2841 ± 10 Ma (Archean). There are prominent Cretaceous and Triassic populations. The Cretaceous peak is the largest with a major peak between 110 and 130 Ma. There are a small number of Jurassic and Permian to Cambrian ages. Precambrian grains are abundant with peaks at c. 0.55, 1.1 and 1.8

Ga. Mesozoic zircon grains are predominantly euhedral and subrounded, while Proterozoic and Archean grains are mostly rounded.

74 concordant U-Pb ages were obtained from 92 zircon grains of sample TB179a from the upper part of the Layar Member (Fig. 11). There are 41 Phanerozoic and 33 Proterozoic ages from 71 ± 1 Ma (Campanian, Late Cretaceous) to 2617 ± 33 Ma (Archean). There is a large Cretaceous population with prominent peaks at 80-90 Ma and 110-130 Ma. A mainly Triassic population is present at 200-260 Ma. There are a few Jurassic, Permian, and Devonian to Cambrian grains. Precambrian grains account for almost 45% of the total number of grains. Proterozoic ages have prominent peaks at c. 0.55, 0.8, 1.1, 1.8, and 2.5 Ga.

7.2.2. Lower Kapit Member

118 concordant U-Pb ages were obtained from 124 grains (Fig. 11) in the western lower Kapit Member sample (TB189a). There are 79 Phanerozoic and 40 Proterozoic ages from 50.7 ± 0.7 (Early Eocene) to 3004 ± 78 Ma (Archean). Again the sample is noteworthy for the almost 33% of Precambrian grains. Like samples from the Layar Member there is a large Cretaceous population with prominent peaks between 80-150 Ma with maximum at 90-110 Ma and a smaller Permo-Triassic population. There are a small number of Jurassic grains, one Ordovician and one Cambrian grain. Precambrian ages have peaks at c. 0.55, 0.8-1.3, 1.5-2.0, and 2.5-2.6 Ga. Mesozoic grains, particular Cretaceous, are euhedral and show only minor rounding. Precambrian grains are usually subrounded to well-rounded and often have a pinkish colour.

7.2.3. Upper Kapit Member

109 concordant U-Pb ages were obtained from 117 grains from sample TB238 (Fig. 12). There are 83 Phanerozoic and 26 Proterozoic ages from 83 ± 1 Ma (Santonian, Late Cretaceous) to 2595 ± 36 Ma (Archean). This is the lowest sample in a group dominated by Cretaceous and Jurassic ages with few Permo-Triassic grains compared to stratigraphically lower samples. There is a major Cretaceous population with a peak between 110-120 Ma and a smaller Jurassic population at 140-160 Ma. There is a small Permian-Triassic population between 220-310 Ma and a number of Paleozoic ages from Carboniferous to Cambrian with a small Silurian peak at c. 430-440 Ma. Precambrian ages are similar to stratigraphically lower samples, but in reduced numbers and only 22% of the grains are Precambrian. Proterozoic ages have only one peak at c. 1.8 Ga. Grains are predominantly subrounded and euhedral.

The change towards a Cretaceous-dominated population continues in TB43b (Fig. 12), sampled almost at the top of the Kapit Member. A total of 57 concordant U-Pb ages were obtained from 78 grains which range from 50 ± 4 Ma (Early Eocene) to 491 ± 4 Ma (Cambrian). Sample TB43b contains

predominantly Cretaceous zircons with a major peak at c. 120 Ma and a moderate number of Jurassic grains (140-200 Ma). There is a small number of Triassic to Cambrian grains with a minor peak at 420 Ma. In contrast to the samples lower in the Rajang Group there are no Precambrian grains. Most grains are euhedral with only minor rounding.

7.2.4. Pelagus Member

Two samples of the Pelagus Member were analysed; one from the western road section (TB193) and one from the interior (TB241). Both samples are dominated by Cretaceous ages (Fig. 12) and are similar to sample TB43b of the upper Kapit Member. 109 concordant U-Pb ages from 118 grains of sample TB193 range from 41 ± 1 Ma (Middle Eocene) to 1992 ± 94 (Paleoproterozoic). 90 concordant U-Pb ages from 113 grains were obtained from sample TB241 ranging from 78 ± 2 Ma (Stage, Late Cretaceous) to 2465 ± 91 Ma (Paleoproterozoic). Apart from Cretaceous ages there are a small number of Jurassic and Permian-Triassic ages, and a few older Phanerozoic grains. The samples are distinctive because of the very small numbers of Precambrian ages (6%). The zircons are usually euhedral with a few subrounded grains.

7.2.5. Metah Member

Samples TB203a and TB195 from the Metah Member were collected on the western road section. In contrast to the upper Kapit and Pelagus Member it contains diverse zircon age populations (Fig. 13), and resembles the lower group of samples from the Lupar Formation and the Layar and lower Kapit Members.

98 concordant ages were obtained from 104 grains in TB203a (Fig. 13) in which the youngest grain is Middle Eocene (44.4 ± 0.6 Ma) and the oldest 2724 ± 90 Ma (Archean). The most prominent populations are Cretaceous with a peak at 90-120 Ma with a Permo-Triassic population with a peak at 210-260 Ma. The Permo-Triassic population is larger than the Cretaceous population. There are a few Jurassic grains and a small number of grains from Carboniferous to Ordovician. The sample has a high proportion of Precambrian ages (36% of the grains analysed). The major peak at 1.8 Ga is accompanied by widely scattered Proterozoic and Archean ages.

Sample TB195 yielded 121 concordant ages from 129 grains (Fig. 13). There are 81 Phanerozoic, 34 Proterozoic and 6 Archean ages from the youngest age of 81 ± 1 Ma (Campanian, Late Cretaceous) to the oldest age of 2706 ± 8 Ma (Archean). Like TB203a the most prominent populations are Cretaceous with a peak at 90-120 Ma and a Permo-Triassic population with a peak at 210-260 Ma. The Permo-Triassic population is similar in numbers to the Cretaceous population. There is also a small Late Jurassic peak. Minor Paleozoic ages range from Permian to Ordovician, with a small Silurian peak. The Precambrian ages have a major peak at 1.8 Ga accompanied by smaller peaks 0.8-

0.9, 1.7 and 2.5 Ga. Both samples are dominated by subrounded to rounded zircons. Mesozoic zircons are both euhedral and subrounded. Proterozoic zircons are mainly well-rounded.

7.2.6. Bawang Member

Sample TB199a was collected from the Bawang Member of the Belaga Formation in the Tatau area below the unconformity overlain by the Tunggal-Rangsi Conglomerate. Sample TB47 came from the Bawang Member in the Sungai Bawang area. The Bawang Member samples contrast sharply with the Metah Member samples, but resemble the upper Kapit and Pelagus Member samples, in being dominated by Cretaceous zircons with very few Precambrian grains (Fig. 13).

141 concordant ages were obtained from 141 grains in sample TB47 (Fig. 13). There are 133 Phanerozoic and only 8 Precambrian ages with a youngest age of 79 ± 1 Ma (Campanian, Late Cretaceous) and an oldest age of 2450 ± 11 Ma (Paleoproterozoic). Cretaceous-Jurassic and Triassic ages are the most abundant. The Cretaceous has a major peak between 110 and 130 Ma and the Triassic at c. 230 Ma. Between them is a Late Jurassic peak at 150-170 Ma. The few Proterozoic ages have a peak at c. 1.8 Ga.

110 concordant U-Pb ages were obtained from 114 zircon grains of sample TB199a (Fig. 13). There are 100 Phanerozoic and 10 Proterozoic ages ranging from 103 ± 2 Ma (Albian, Early Cretaceous) to 1886 ± 11 Ma (Paleoproterozoic). An Early Cretaceous population has a major peak between 120 and 140 Ma and there is a Jurassic population with a major peak between 150 and 160 Ma. There are a small number of Triassic grains and one Cambrian grain. Like TB47 the few Proterozoic ages have a peak at c. 1.8 Ga. The Cretaceous and Jurassic zircons are dominated by subrounded and rounded grains with a small number of euhedral zircons, indicating recycling of most grains. Older grains are typically subrounded to rounded and are interpreted to indicate multiple recycling.

8. Discussion

8.1. Depositional environment, deformation and metamorphism

The original mapping of the Rajang Group showed it had a deep marine character (Haile, 1957; Kirk, 1957; Wolfenden, 1960; Liechti et al., 1960). The Rajang Group is now interpreted to be dominated by turbidites (Hutchison, 1996) deposited in a submarine fan (Tongkul, 1997; Bakar et al., 2007). Observations made during this study support these interpretations. Turbidite sandstones have scoured bases, grading and parallel lamination. Linked debrites are commonly represented by amalgamated sandstones with mud clasts. Macrofossils and microfossils are rare which may indicate a stressed environment or they may have been removed during deformation or metamorphism.

Slump structures and other indications of syn-sedimentary deformation are common. Wolfenden (1960) observed that deformation in the Rajang Group could not be due to a single orogenic event and may be related to syn-depositional deformation. Large folds are common and are interpreted as slump structures resulting from gravity-driven syn-depositional movements on slope. Bakar et al. (2007) reported deformation features to be more common in the older Pelagus Member near Sibu compared to parts of the Belaga Formation further north in the Tatau region (Metah and Bawang Members).

The main differences are small variations in sandstone abundance and type. The Pelagus Member is more arenaceous whereas the Layar, Kapit, Metah and Bawang Members are generally shale dominated. The interior of Sarawak remains remote, largely inaccessible and almost uninvestigated since the pioneering work of the 1950s and 1960s but fieldwork during this study and SRTM images suggest thicker and more proximal sandstone bodies there, compared to exposures close to the coast. The western exposures sampled in this study are typically thinner bedded and have a more distal character than outcrops in the interior where thick amalgamated sandstone packages indicate high sedimentation rates with sedimentary structures indicating rapid deposition. This indicates a transition from proximal to distal from east to west within the Rajang Group. Thus, the main input of sediment is likely to have been from the south and southeast.

A large part of the Rajang Group has undergone low grade metamorphism. The Lupar Formation, Layar and Kapit Members typically consist of indurated metasandstones and low grade schists. Cleavage is well developed and quartz veining is common, especially in the Lupar Formation and Layar Member. Metamorphism becomes less obvious in the Pelagus and Metah Members, and cleavage and quartz veining become subordinate to absent in the upper members of the Rajang Group. There is also an apparent along-strike trend from west to east towards a higher grade of metamorphism in the interior of the Sibu Zone in contrast to western sections.

It is noteworthy that the isolated northernmost exposures of the Rajang Group assigned to the Bawang Member are indurated metasandstones and well cleaved phyllites. This is inconsistent with the inferred young age of this member.

8.2. New subdivisions

As observed above, the Rajang Group has been described as a monotonous flysch group locally metamorphosed to lower greenschist facies (Hutchison, 1996). In the original mapping it was recognised that identification of different members was only approximately possible, and was based partly on lithological characteristics and partly on limited paleontological data (Liechti et al., 1960). Subdivision of the Rajang Group in the field remains difficult. Fossils are rare, and low grade

metamorphism means microfossils are unlikely to be found in pelitic beds. Sandstones have similar quartz-rich compositions and lithological differences mainly reflect variations in depositional environments in a long-lived submarine fan, modified by tropical processes. However, the heavy mineral assemblages and detrital zircon ages do provide the basis for subdivision of the Rajang Group, which is largely consistent with the ages previously proposed, offer answers to some speculations about previous uncertainties in stratigraphy, and give insights into changing sediment sources from the Late Cretaceous to Late Eocene. These units proposed in this study are consistent with the original mapping and dating by Milroy (1953), Haile (1957), Kirk (1957), Wolfenden (1960) and Liechti et al. (1960).

We propose a new three-fold classification of the Rajang Group based on heavy mineral assemblages and detrital zircon ages. Table 4 summarises the new subdivisions of the Rajang Group. Unit 1 is composed of the Lupar Formation, Layar Member and lower part of the Kapit Member. Unit 2 is exposed north of the Rajang River and includes the upper Kapit Member and the Pelagus Member. Unit 3 is the Metah Member in the northernmost part of the Rajang Group in the Sibu Zone. The Bawang Member is exposed in windows within the Miri Zone separated from the rest of the Rajang Group in the Sibu Zone and is discussed further below, but we consider it to be probably the equivalent of Unit 2, but possibly an equivalent of Unit 1. It is not an equivalent of the Metah Member (our Unit 3) as previously speculated and is not the youngest part of the Rajang Group. Fig. 14 displays a SRTM image of the Sibu Zone showing the distribution of the proposed units. The boundary between Units 1 and 2 is in an area between the Sebangkoi lineament and the Rajang River lineament which is unsampled because of lack of exposures. The top of Unit 2 is the Bakun lineament (named here after the Bakun dam). The Bukit Mersing Line marks the top of Unit 3 and also the boundary with the Miri Zone.

8.3. Heavy Minerals

Heavy mineral assemblages are dominated by the ultra-stable minerals zircon, tourmaline and rutile, with small percentages of garnet, chlorite, apatite, epidote and rare chrome spinel. The three units have distinctive heavy mineral assemblages. Unit 1 has a zircon-dominated assemblage in the single sample of the Lupar Formation at the base, but other samples are characterised by a tourmaline+zircon-dominated assemblage. In Unit 2 zircon is the most abundant heavy mineral, and tourmaline is less abundant, but the subsidiary heavy minerals are more varied than in Unit 1 and there is more garnet and apatite. Unit 3 resembles Unit 1 in its tourmaline+zircon-dominated assemblage. The heavy mineral assemblage of the Bawang Member is zircon-dominated, and resembles Unit 2 and the Lupar Formation at the base of Unit 1.

8.4. Depositional ages

8.4.1. Unit 1

Lupar Formation

Maastrichtian foraminifera ages were reported by Milroy (1953) and Tan (1979). The sample from the lower part of the Lupar Formation and therefore the lowermost part of the Rajang Group has a minimum depositional age, based on the youngest zircon, of 70 ± 1 Ma (Maastrichtian, Late Cretaceous). Other Late Cretaceous zircons are Campanian (84-72 Ma).

Layar Member

Liechti et al. (1960) suggested an age range of Turonian to Maastrichtian for the Layar Member supported later by foraminifera data (Tan, 1979). Hutchison (2005) argued that the foraminifera data used by Liechti et al. (1960) suggested a Cenomanian to Turonian age. The youngest zircon age from the Layar Member of 71 ± 1 Ma indicates a minimum depositional age of Maastrichtian, similar to the Lupar Formation sample. Abundant Campanian zircons confirm the Late Cretaceous age. This clearly rules out Hutchison's proposal and supports the age estimates of Liechti et al. (1960) and Tan (1979).

Lower Kapit Member

A Paleocene to Early Eocene age was assigned to the Kapit Member based on foraminifera (Wolfenden, 1960; Liechti et al., 1960). The youngest zircons from the lower Kapit Member are Early Eocene (50.7 ± 0.7 Ma). Other Cenozoic zircons are of Paleocene age.

8.4.2. Unit 2

Upper Kapit Member

The youngest zircon from the upper Kapit Member is Early Eocene (50 ± 4 Ma in sample TB43b) similar to the lower Kapit Member.

Pelagus Member

The Pelagus Member was suggested by Liechti et al. (1960) to be Middle to Upper Eocene. Hutchison (2005) used data from Wolfenden (1960) to suggest that the Pelagus Member was Lower to Middle Eocene. The youngest zircons dated in this study from the Pelagus Member are 41 ± 1 Ma (Middle Eocene). This age is consistent with the interpretations of both Liechti et al. (1960) and Hutchison (2005).

8.4.3. Unit 3

Metah Member

Based on paleontological work by Liechti et al. (1960) and Wolfenden (1960) the Metah Member was considered to be younger than the Pelagus Member and suggested to be Upper Eocene, although neither member was very precisely dated. Hutchison (2005) suggested the Metah Member was Middle to Upper Eocene, based on paleontological data from Kirk (1957). The youngest zircon from the Metah Member is 44.4 ± 1.3 Ma (Middle Eocene) which is slightly older than the youngest zircon (41 ± 1 Ma) from the underlying Pelagus Member. The zircon ages cannot distinguish between the different interpretations of Liechti et al. (1960) and Hutchison (2005).

8.4.4. Bawang Member

The stratigraphic position of the Bawang Member is unknown as no age diagnostic fossils have been found in it but it was speculated to be an equivalent of the Metah Member (Liechti et al., 1960). The youngest zircon of the Bawang Member is 76 ± 1 Ma and significantly older than the youngest zircon in the Metah Member. The zircon age populations from the Bawang Member samples are distinctive and quite different from the Metah Member (Fig. 13). They resemble those of Unit 2 (Pelagus and upper Kapit Member) in the abundance of Cretaceous zircons with very few Precambrian grains. TB199a is almost identical to Pelagus Member samples, but TB47 has a large number of Triassic zircons similar to those found, although less abundantly, in Units 1 and 3 (Lupar Formation, Layar, Kapit and Metah Members). However, abundant Triassic zircons in those samples are usually accompanied by Permian, older Paleozoic and large numbers of Precambrian grains, which is not the case for TB47. The Bawang Member samples also differ from other Rajang Group samples in having a relatively large number of Jurassic zircons. The zircon ages indicate only a maximum depositional age of Late Cretaceous (Campanian) for the Bawang Member and do not resolve its stratigraphic position in the Rajang Group. However, the detrital zircon ages indicate it is unlikely to be a deeper water equivalent of the Metah Member as speculated by Liechti et al. (1960). As noted above, the presence of a cleavage in the Bawang Member is also inconsistent with a young age for the Metah Member.

8.5. Provenance and sources

Most sandstones are quartz-dominated, with abundant lithic fragments of plutonic, volcanic, metamorphic or sedimentary origin and both feldspar varieties. The conventional light mineral plots indicate a recycled orogenic provenance (Fig. 7) for most samples, but they give little insight into likely sources beyond this. Furthermore, feldspar dissolution and breakdown of unstable lithic

fragments during transport, erosion and alluvial storage of sand in a humid tropical environment (Suttner et al., 1981; Johnsson et al., 1988; Smyth et al., 2008; van Hattum et al., 2013) may have altered the original composition significantly.

All samples from the Rajang Group are dominated by ultra-stable heavy minerals that indicate a predominantly acid granitic source with a subsidiary metamorphic contribution. Zircons are the most abundant heavy mineral in most samples. Rounded zircons with frosted surfaces and Paleozoic to Precambrian ages indicate a recycled sedimentary provenance, whereas euhedral and subhedral grains with Mesozoic ages are likely to have been derived directly, or with little recycling, from acid igneous source rocks. The few chrome spinel grains in a small number of samples indicates very minor input from ultrabasic/ophiolitic rocks. These could have been derived from rocks of the Lubok Antu Melange now exposed in the Lupar Valley, also no ultramafic rocks are exposed (Haile et al., 1994) or from the Boyan Melange that potentially underlie the Rajang Group. The dominance of ultra-stable heavy minerals shows a compositional maturity which could be related to multiple recycling, acid dissolution during transport and deposition or diagenesis, or low-grade metamorphic processes, removing less stable minerals. The abundance of rounded zircon and tourmaline indicates significant recycling.

The two dominant Phanerozoic age populations in the Rajang Group sandstones are Cretaceous and Triassic but there are a few Paleogene grains in most samples.

8.5.1. Paleogene zircons

Paleogene zircons are likely derived from contemporaneous magmatism in Borneo. K-Ar ages reported by Pieters et al. (1987), Bladon et al. (1989), de Keyser and Rustandi (1993), Pieters and Sanyoto (1993) and Pieters et al. (1993) indicate minor localised magmatism in Central Borneo. The very small number of Paleogene zircons indicates very limited magmatism at the time of deposition. Therefore a submarine fan derived from an active subduction margin as shown in the model of Hutchison (1996, 2005) is not supported. A much more diverse heavy mineral assemblage and immature light mineral composition would also be expected if the Rajang Group was sourced by an active magmatic arc.

8.5.2. Cretaceous zircons

The Schwaner Mountains region was potentially a major source for the Rajang Group. K-Ar ages from volcanic and magmatic rocks of the Schwaner Mountains were reported by Haile et al. (1977) and Williams et al. (1988). Almost all zircons from the extensive granites of the Schwaner Mountains and from the Pinoh Metamorphics in SW Borneo (Fig. 15) are Cretaceous (Davies, 2013; van Hattum et al., 2013; Davies et al., 2014; Hennig et al., 2017). Ages range from c. 130 to 80 Ma which matches

well the Cretaceous zircon population in the Rajang Group. A distinctive feature of the Schwaner region is the absence of Precambrian zircons. This also matches well to Unit 2, which could therefore be explained by a single source.

Cretaceous granites of the Malay Peninsula are typically about 90 to 80 Ma (Searle et al., 2012; Cottam et al., 2013) and could not account for the large number of older Cretaceous zircons in the Rajang Group.

Abundant Cretaceous magmatism is reported from the Da Lat Zone in SE Vietnam (Nguyen et al., 2004; Shellnut et al., 2013), and interpreted as the continuation of the same Paleo-Pacific subduction magmatism that formed the Schwaner Mountain granites (Breitfeld et al., 2017; Hennig et al., 2017). However, considering the distance from Sarawak we suggest it is unlikely that significant input was derived from SE Vietnam (Fig. 15).

8.5.3. Jurassic zircons

Jurassic zircons that accompany Cretaceous zircons in smaller numbers could also be derived from Borneo. Haile et al. (1977), van Hattum et al. (2013) and Davies et al. (2014) identified Jurassic magmatism in the southern Schwaner Mountains. Hennig et al. (2017) reported Jurassic magmatism in West Borneo (NW Schwaner Zone). Alternatively, Jurassic zircons could have been derived from the Malay Peninsula. Clements et al. (2011) suggested that the Khorat Group of Thailand (Carter and Moss, 1999) could have extended from Indochina into the Malay Peninsula where remnants of terrestrial red beds are found locally (Fig. 15).

8.5.4. Triassic zircons

The area of NW Kalimantan and West Sarawak is the closest potential source for Triassic zircons in the Rajang Group. Breitfeld et al. (2017) dated abundant Upper Triassic zircons from the Jagoi Granodiorite and Triassic clastic sediments of the Sadong and Kuching Formations in West Sarawak. Hennig et al. (2017) reported Triassic zircons from the northwestern Schwaner Mountains in Kalimantan. Setiawan et al. (2013) suggested input of Triassic material from southern Borneo.

Other Triassic exposures in Borneo include the Busang Complex (Williams et al., 1988) interpreted as allochthonous by Hennig et al. (2017). However, the size of the Busang Complex is too small to account for significant input and it is also uncertain if the Busang Complex was exposed during the Cenozoic.

An obvious potential source for Triassic zircons is the well-known and extensive Tin Belt granites of the Malay Peninsula (Hutchison, 1977; Cobbing et al., 1986; Hutchison and Tan, 2009; Cottam et al. 2013). Searle et al. (2012) reported abundant Permian-Triassic zircons from granites. Detrital

Permian-Triassic zircons are abundant in modern river sands of the Malay Peninsula (Sevastjanova et al., 2011). Van Hattum (2005) and van Hattum et al. (2006, 2013) suggested the Malay Peninsula was the main source of Permo-Triassic zircons in the Crocker and Sapulut Formations in NW Sabah. However, brown zircons are abundant in the Malay Peninsula and considered to be diagnostic of this source region (Krähenbuhl, 1991; Sevastjanova, 2007), but are rare in the Belaga Formation and this may indicate only limited input from there.

Indochina and SE China are possible source regions. Triassic zircons are reported from the Kontum massif in Vietnam (Lan et al., 2003; Hieu et al., 2015) and central Vietnam/Laos/SE China/Hainan (Liu et al., 2012; Vladimirov et al., 2012; Mao et al., 2013; Ishihara and Orihashi, 2014; Jiang et al., 2015; Halpin et al., 2016; Wang et al., 2016; Yan et al., 2017). Burrett et al. (2014) reported abundant Permian-Triassic zircons from northern Thailand and Arboit et al. (2016) from central Thailand. Usuki et al. (2013) demonstrated the central part of Vietnam (NE Indochina) has a slightly different zircon signature compared to the rest of Indochina, thus indicating if zircons were sourced from Indochina, they were not derived from the northern part. The distance from north and northwest Indochina to the Rajang Group is significant (Fig. 15) and a northern source is also inconsistent with the east to west change from proximal to distal deposits in the fan, which indicates a southern input of sediment. Thus, it is unlikely that these regions represented a major direct source.

8.5.5. Precambrian zircons

The immediate source of the various Precambrian grains is difficult to interpret as these have clearly been reworked during multiple cycles. Breitfeld et al. (2017) reported abundant c. 1.8 Ga and some c. 2.5 Ga zircons from the Triassic Kuching and Sadong Formations of West Sarawak. However, there are almost no other Precambrian zircons in these formations and other sources are required to explain the diverse Precambrian zircon populations within the Rajang Group. The Cretaceous Pedawan Formation of West Sarawak and NW Kalimantan has slightly more diverse Precambrian zircon ages (Breitfeld et al., 2017) and could be a potential nearby source.

Similar Paleoproterozoic zircon populations are also common in SE China (Liu et al., 2009; Chen and Xing, 2013; Chen et al., 2016; Xu et al., 2016), East Malaya (Sevastjanova et al., 2011) and Vietnam (Lan et al., 2001, 2003). Carter and Moss (1999) reported 1.8 Ga and 2.5 Ga zircons from the Khorat Group in Thailand and Hara et al. (2013) dated detrital zircons of similar age from northern Thailand, but other Precambrian ages are rare.

The most important Precambrian zircon age populations, besides 1.8 Ga and 2.5 Ga, in the Rajang Group are c. 500 Ma, 800 Ma and 1.2 Ga. Abundant zircons of these ages are reported from Phuket Island, southern Thailand (Burrett et al., 2014) and from central Thailand (Arboit et al., 2016). These

766 populations are also common in Cenozoic sediments in other parts of Sundaland. Clements and Hall
767 (2011) reported them from West Java, part of SW Borneo and Smyth et al. (2007) from East Java. A
768 Triassic sandstone from Sibumasu has comparable Precambrian zircon populations (Hall and
769 Sevastjanova, 2012), which could indicate that Precambrian zircons in the Rajang Group were
770 recycled from Sibumasu. Smyth et al. (2007) suggested that the East Java zircons were derived from
771 the Pinjara (500-800 Ma) and Albany-Fraser (1000-1300 Ma) orogens of western Australia.

772 *8.6. Paleogeography*

773 This study shows that the Rajang Group in Sarawak consists of three units with distinctive
774 provenance characteristics that indicate shifts in source material through time. Unit 1 was derived
775 from SW Borneo (Schwaner Mountains) and Sundaland (West Borneo or Malay Tin Belt), whereas
776 Unit 2 was sourced almost entirely from SW Borneo. Unit 3 was derived from a SW Borneo and
777 Sundaland source. Lower Mesozoic, Paleozoic and Precambrian zircons are usually subrounded to
778 rounded and indicate recycling from older sediments as important source. With time, the relative
779 importance of the two major sources fluctuated.

780 Based on the results in this study and previous paleontological dating, it is clear that the fan system
781 was active for at least 30 Ma from the Maastrichtian to the Middle/Late Eocene, with a major
782 contribution from southern Borneo. Massive amounts of sediment must have been transported by a
783 large river system. The actual observable fan size comprises the whole Sibu Zone (Central Sarawak)
784 with a length of c. 140 km and a width of c. 450 km, covering an area of c. 6.3×10^4 km^2. The Rajang
785 Group extends into north Sarawak and Sabah with equivalents in the Mulu and the Sapulut
786 Formations (Haile, 1962; Collenette, 1965; Tate, 1991). This indicates a much larger possible fan
787 width of up to c. 850 km and an area of c. 1.2×10^5 km^2. The Rajang Group also extends westwards
788 beneath offshore Sarawak (Madon, 1999; Mat-Zin, 2000) and could cover an even larger area. This
789 would make the Rajang Group submarine fan one of the largest ancient fans in the world (see
790 comparative data in Shanmugam, 2016). It is similar in size to some modern deep water fan systems
791 such as the Amazon, the Laurentian and the Mississippi (Shanmugam, 2016).

792 Fig. 15 displays the interpreted depositional area and provenance of the Rajang Group based on the
793 results of this study. During the Early Cretaceous, SW Borneo had been added to Sundaland (Hall,
794 2012; Hennig et al., 2017) and the Sibu Zone (Central Sarawak) was situated at the Sundaland margin
795 in the Late Cretaceous (Breitfeld et al., 2017). The Lupar Line probably formed the shelf edge with
796 mainly terrestrial sedimentation to the south, where sediments of the Kuching Zone were deposited
797 in a number of strike-slip basins, and the Rajang Group deep water fan to the north. We suggest the
798 Lupar Line was an important left-lateral strike-slip fault active during the deposition of the Rajang

Group and it could have linked to the latest Cretaceous to early Cenozoic thrusting in the Kampot Fold Belt in SW Vietnam described by Fyhn et al. (2016).

Our results support models by Tan (1982) and Williams et al. (1988) that suggest a southern source in Borneo. Sediment was derived from an elevated landmass to the south or southwest, eroding mostly acid igneous (granitic) material. The Schwaner Mountains in SW Borneo and the area of NW Kalimantan and West Sarawak are therefore likely source areas. The Schwaner granites and possible sedimentary cover are the most likely source of Cretaceous zircons. Triassic zircons are most likely to have come from the Malay Peninsula but the relatively small number of brown zircons, which are typical of the Malay Peninsula granites, indicates a smaller contribution as suggested by van Hattum et al. (2013). Zircon age populations, especially in Unit 2, resemble the Lower Eocene Sapulut Formation in Sabah but its heavy mineral assemblage also includes apatite, garnet, tourmaline and chrome spinel with pyroxene, amphibole and chloritoid (van Hattum, 2005; van Hattum et al., 2013). This more immature assemblage probably reflects an important local ophiolite source in Sabah.

It is unlikely that Indochina or SE China was a direct source of sediment, e.g. via a proto-Mekong River (e.g. Hutchison, 1996), considering the distance to Sarawak and the fact that the great rivers flowing through Indochina result from much later India-Asia collision. Clements et al. (2011) suggested a former larger extent of the Khorat Basin into the Gulf of Thailand and the Malay Peninsula from which zircons with Indochina signature could have been recycled into the Rajang Group (Fig. 15).

There is little evidence to support the suggestion by Hutchison (1996) that the Rajang Group is an accretionary prism formed by south-directed subduction. Although zircons close to the depositional age indicated by fossils are found in most samples, showing some contemporaneous magmatism, they are not as abundant as would be expected from a subduction arc. Deformation and metamorphism of the fan do not require collision and subduction. A plausible present-day equivalent of the Rajang Group is the fold and thrust belt of offshore NW Sabah. Major toe-thrust deformation is caused by down-slope gravity-driven collapse. The deformation observed in the deep water sediments is attributed to syn-depositional processes (Hesse et al., 2010), such as large-scale submarine landslides (Gee et al., 2007; Morley, 2007a), slumps and slides (McGilvery and Cook, 2003; Morley, 2007b, 2009). Significant sub-surface deformation and low grade metamorphism is likely in the deeper parts of the sediment wedge. Studies of the offshore Niger delta (e.g. Corredor et al., 2005) show extensional faults and thrusts at depths of several kilometres, where low grade metamorphism would be expected. Deformation and development of cleavage within the Mesa Central submarine fan in Mexico (Silva-Romo et al., 2000) is associated with displacement along a

major strike-slip fault. The Lupar Line could also be responsible for some deformation in the Rajang Group.

Our results indicate the change in Sarawak from deep marine to terrestrial sedimentation marked by the Rajang Unconformity occurred in the late Middle Eocene (approximately 40 Ma). After that time onshore and offshore Sarawak was a shallow marine shelf. Uplift of the Rajang Group to form the mountainous region of present-day central Borneo must have occurred relatively recently. Further studies of the Neogene in NW Borneo are required to analyse this uplift history.

9. Conclusions

The Rajang Group is a large submarine fan, active for approximately 30 to 40 Ma, comparable in size to major modern fans. It is dominated by turbidite deposits and debrites showing locally significant syn-sedimentary deformation. The previous established subdivision into members based on slight lithological differences is hard to apply. We propose a new three unit classification based on heavy minerals and detrital zircon ages to subdivide a monotonous deep water sequence and show changes in source in time.

Heavy minerals are dominated by ultrastable varieties. They indicate sources for the Rajang Group were predominantly acid igneous rocks with subsidiary metamorphic and reworked sedimentary rocks. There was very little input from ultrabasic/ophiolitic sources. Major sources for the Rajang Group were the Schwaner Mountains in SW Borneo, Mesozoic clastic sediments and igneous rocks of West Borneo and the Tin Belt of Sundaland. The importance of these sources fluctuated with time.

The material derived from West Borneo and the Tin Belt is characterised by a mature tourmaline-rutile-zircon heavy mineral assemblage. Detritus derived from the Schwaner Mountains was dominated by zircons. The Bawang Member is not the equivalent of the Metah Member. This study suggests that it is likely to be an equivalent of Unit 2 (Pelagus Member) or less probably the base of Unit 1 (Lupar Formation).

Although rare zircons throughout the sequence indicate contemporaneous magmatism, the Rajang Group was not formed in an active subduction margin setting. Intermittent magmatism in Borneo is known throughout the Cenozoic and has continued in Sarawak at least into the Pliocene but the cause is not clear.

Acknowledgements

We thank editor Sanghoon Kwon and reviewers Clive Burrett and Chris Morley for helpful comments that improved the manuscript. This project was funded by the SE Asia Research Group of Royal

Holloway University of London, which is supported by a consortium of oil companies. The Economic Planning Unit of Malaysia and the State Planning Unit of Malaysia made the fieldwork possible, and the Mineral and Geoscience Department Malaysia, Sarawak assisted in the field and with the logistics. Richard Mani Banda was especially helpful. We thank Juliane Hennig for helpful discussions, Martin Rittner and Andy Carter (UCL/Birkbeck College) for help and support at the LA-ICP-MS facility, Andy Beard (UCL/Birkbeck College) and Dominique Tanner (Royal Holloway University) for help with cathodoluminescence imaging.

References

Allen, J.R.L., 1964. Studies in fluviatile sedimentation: six cyclothems from the Lower Old Red Sandstone, Anglowelsh Basin. Sedimentology 3, 163-198.

Andersen, T., 2002. Correction of common lead in U–Pb analyses that do not report 204 Pb. Chemical Geology 192, 59-79.

Arboit, F., Collins, A.S., Morley, C.K., King, R. and Amrouch, K., 2016. Detrital zircon analysis of the southwest Indochina terrane, central Thailand: Unravelling the Indosinian orogeny. Geological Society of America Bulletin 128, 1024-1043.

B.R.G.M., 1982. Geological mapping and mineral exploration in northeast Kalimantan, 1979–1982. Final report. Rapport du Bureau de Recherches géologique et minières 82 RDM 007AO.

Bakar, Z.A.A., Madon, M. and Muhamad, A.J., 2007. Deep-marine sedimentary facies in the Belaga Formation (Cretaceous-Eocene), Sarawak: Observations from new outcrops in the Sibu and Tatau areas. Geological Society of Malaysia Bulletin 53, 35 – 45.

Bladon, G.M., Pieters, P.E. and Supriatna, S., 1989. Catalogue of isotopic ages commissioned by the Indonesia-Australia Geological Mapping Project for igneous and metamorphic rocks in Kalimantan, Preliminary Report. Geological Research and Development Centre, Bandung.

Breitfeld, H.T., Hall, R., Galin, T., Forster, M.A. and BouDagher-Fadel, M.K., 2017. A Triassic to Cretaceous Sundaland–Pacific subduction margin in West Sarawak, Borneo. Tectonophysics 694, 35-56.

Burrett, C., Zaw, K., Meffre, S., Lai, C.K., Khositanont, S., Chaodumrong, P., Udchachon, M., Ekins, S. and Halpin, J., 2014. The configuration of Greater Gondwana—evidence from LA ICPMS, U–Pb geochronology of detrital zircons from the Palaeozoic and Mesozoic of Southeast Asia and China. Gondwana Research 26, 31-51.

Carter, A. and Moss, S.J., 1999. Combined detrital-zircon fission-track and U-Pb dating: A new approach to understanding hinterland evolution. Geology 27, 235–238.

Chen, Z.-H. and Xing, G.-F., 2013. Petrogenesis of a Palaeoproterozoic S-type granite, central Wuyishan terrane, SE China: implications for early crustal evolution of the Cathaysia Block. International Geology Review 55, 1445-1461.

Chen, Z.-H., Xing, G.-F. and Zhao, X.-L., 2016. Palaeoproterozoic A-type magmatism in northern Wuyishan terrane, Southeast China: petrogenesis and tectonic implications. International Geology Review 58, 773-786.

Clements, B., Burgess, P.M., Hall, R. and Cottam, M.A., 2011. Subsidence and uplift by slab-related mantle dynamics: a driving mechanism for the Late Cretaceous and Cenozoic evolution of continental SE Asia? Geological Society, London, Special Publications 355, 37-51.

Clements, B. and Hall, R., 2011. A record of continental collision and regional sediment flux for the Cretaceous and Palaeogene core of SE Asia: implications for early Cenozoic palaeogeography. Journal of the Geological Society 168, 1187-1200.

Cobbing, E.J., Mallick, D.I.J., Pitfield, P.E.J. and Teoh, L.H., 1986. The granites of the Southeast Asian tin belt. Journal of the Geological Society 143, 537-550.

Collenette, P., 1965. The geology and mineral resources of the Pensiangan and Upper Kinabatangan area, Sabah. Malaysia Geological Survey Borneo Region, Memoir 12, 150.

Corredor, F., Shaw, J.H. and Bilotti, F., 2005. Structural styles in the deep-water fold and thrust belts of the Niger Delta. AAPG Bulletin 89, 753-780.

Cottam, M.A., Hall, R. and Ghani, A.A., 2013. Late Cretaceous and Cenozoic tectonics of the Malay Peninsula constrained by thermochronology. Journal of Asian Earth Sciences 76, 241-257.

Cullen, A., Macpherson, C., Taib, N.I., Burton-Johnson, A., Geist, D., Spell, T. and Banda, R.M., 2013. Age and petrology of the Usun Apau and Linau Balui volcanics: Windows to central Borneo's interior. Journal of Asian Earth Sciences 76, 372-388.

Cummins, W.A., 1962. The greywacke problem. Geological Journal 3, 51-72.

Davies, L., Hall, R. and Armstrong, R., 2014. Cretaceous crust in SW Borneo: petrological,

922 geochemical and geochronological constraints from the Schwaner Mountains, Proceedings
923 Indonesian Petroleum Association, 38th Annual Convention and Exhibition, IPA14-G-025.
924 Davies, L.B., 2013. SW Borneo Basement: Age, origin and character of igneous and metamorphic
925 rocks from the Schwaner Mountains. Ph.D. Thesis, Royal Holloway University of London, 391
926 pp.
927 de Keyser, F. and Rustandi, E., 1993. Geology of the Ketapang Sheet area, Kalimantan. Map at
928 1:250000 scale. Geological Research and Development Centre, Bandung.
929 De Silva, S., 1986. Stratigraphy of south Mukah–Balingian region. Sarawak. Newsl. Geol. Soc.
930 Malaysia 12, 215-219.
931 Dickinson, W.R., 1970. Interpreting detrital modes of graywacke and arkose. Journal of Sedimentary
932 Research 40, 695-707.
933 Dickinson, W.R., Beard, L.S., Brakenridge, G.R., Erjavic, J.L., Ferguson, R.C., Inman, K.F., Knepp, R.A.,
934 Lindeberg, F.A. and Ryberg, P.T., 1983. Provenance of North American Phanerozoic
935 sandstone in relation to tectonic setting. Geological Society of America Bulletin 94.
936 Fyhn, M.B.W., Green, P.F., Bergman, S.C., Van Itterbeeck, J., Tri, T.V., Dien, P.T., Abatzis, I., Thomsen,
937 T.B., Chea, S. and Pedersen, S.A.S., 2016. Cenozoic deformation and exhumation of the
938 Kampot Fold Belt and implications for south Indochina tectonics. Journal of Geophysical
939 Research: Solid Earth 121, 5278-5307.
940 Galehouse, J.S., 1971. Point counting. In: R.E. Carver (Ed.), Procedures in Sedimentary Petrology,
941 Wiley, New York, pp. 385-407.
942 Gazzi, P., 1966. Le arenarie del flysch sopracretaceo dell'Appennino modenese; correlazioni con il
943 flysch di Monghidoro. Mineral. Petrogr. Acta 12, 69-97.
944 Gazzi, P., Zuffa, G.G., Gandolfi, G. and Paganelli, L., 1973. Provenienza e dispersione litoranea delle
945 sabbie delle spiagge adriatiche fra le foci dell'Isonzo e del Foglia: inquadramento regionale.
946 Memorie della Societa Geologica Italiana 12, 1-37.
947 Gee, M.J.R., Uy, H.S., Warren, J., Morley, C.K. and Lambiase, J.J., 2007. The Brunei slide: a giant
948 submarine landslide on the North West Borneo Margin revealed by 3D seismic data. Marine
949 Geology 246, 9-23.
950 Griffin, W.L., Powell, W.J., Pearson, N.J. and O'Reilly, S.Y., 2008. GLITTER: data reduction software for
951 laser ablation ICP-MS. Laser Ablation-ICP-MS in the earth sciences. Mineralogical association
952 of Canada short course series 40, 204-207.
953 Haile, N.S., 1957. The geology and mineral resources of the Lupar and Saribas Valleys, West Sarawak.
954 Malaysia Geological Survey Borneo Region, Memoir 5, 123pp.
955 Haile, N.S., 1962. The geology and mineral resources of the Suai-Baram area, north Sarawak.
956 Geological Survey Department British Territories in Borneo, Memoir 13, 176 pp.
957 Haile, N.S., 1968. The northwest Borneo geosyncline in its geotectonic setting. Bulletin of the
958 Geological Society of Malaysia, Studies in Malaysian Geology 1, 59-60.
959 Haile, N.S., 1974. Borneo. In: A.M. Spencer (Ed.), Mesozoic-Cenozoic Orogenic Belts. Geological
960 Society of London Special Publication 4, pp. 333-347.
961 Haile, N.S., Lam, S.K. and Banda, R.M., 1994. Relationship of gabbro and pillow lavas in the Lupar
962 Formation, West Sarawak: Implications for interpretation of the Lubok Antu Melange and
963 the Lupar Line. Bulletin of the Geological Society of Malaysia 36, 1-9.
964 Haile, N.S., McElhinny, M.W. and McDougall, I., 1977. Palaeomagnetic data and radiometric ages
965 from the Cretaceous of West Kalimantan (Borneo), and their significance in interpreting
966 regional structure. Journal of the Geological Society of London 133, 133-144.
967 Hall, R., 2002. Cenozoic geological and plate tectonic evolution of SE Asia and the SW Pacific:
968 computer-based reconstructions, model and animations. Journal of Asian Earth Sciences 20,
969 353-434.
970 Hall, R., 2012. Late Jurassic–Cenozoic reconstructions of the Indonesian region and the Indian Ocean.
971 Tectonophysics 570–571, 1-41.
972 Hall, R. and Breitfeld, H.T., 2017. Nature and demise of the Proto-South China Sea. Geological Society

of Malaysia Bulletin 63, 61-76.
Hall, R., Clements, B. and Smyth, H.R., 2009. Sundaland: Basement character, structure and plate tectonic development. Proceedings Indonesian Petroleum Association 33rd Annual Convention, IPA09-G-134 1-27.
Hall, R. and Sevastjanova, I., 2012. Australian crust in Indonesia. Australian Journal of Earth Sciences 59, 827-844.
Hall, R., van Hattum, M.W.A. and Spakman, W., 2008. Impact of India-Asia collision on SE Asia: the record in Borneo. Tectonophysics 451, 366-389.
Halpin, J.A., Tran, H.T., Lai, C.-K., Meffre, S., Crawford, A.J. and Zaw, K., 2016. U–Pb zircon geochronology and geochemistry from NE Vietnam: A 'tectonically disputed'territory between the Indochina and South China blocks. Gondwana Research 34, 254-273.
Hamilton, W., 1979. Tectonics of the Indonesian region. U.S.G.S. Prof. Paper 1078, 345pp.
Hara, H., Kon, Y., Usuki, T., Lan, C.-Y., Kamata, Y., Hisada, K.-i., Ueno, K., Charoentitirat, T. and Charusiri, P., 2013. U–Pb ages of detrital zircons within the Inthanon Zone of the Paleo-Tethyan subduction zone, northern Thailand: New constraints on accretionary age and arc activity. Journal of Asian Earth Sciences 74, 50-61.
Hazebroek, H.P. and Tan, D.N.K., 1993. Tertiary tectonic evolution of the NW Sabah Continental Margin. Bulletin of the Geological Society of Malaysia 33, 195-210.
Heng, Y.E., 1992. Geological Map of Sarawak, 1:500,000. Geological Survey of Malaysia.
Hennig, J., Hall, R. and Armstrong, R.A., 2016. U-Pb zircon geochronology of rocks from west Central Sulawesi, Indonesia: Extension-related metamorphism and magmatism during the early stages of mountain building. Gondwana Research 32, 41-63.
Hennig, J., Breitfeld, H.T., Hall, R. and Nugraha, A.M.S., 2017. The Mesozoic tectono-magmatic evolution at the Paleo-Pacific subduction zone in West Borneo. Gondwana Research 48, 292-310.
Hesse, S., Back, S. and Franke, D., 2010. The structural evolution of folds in a deepwater fold and thrust belt - a case study from the Sabah continental margin offshore NW Borneo, SE Asia. Marine and Petroleum Geology 27, 442-454.
Hieu, P.T., Yang, Y.-Z., Binh, D.Q., Nguyen, T.B.T., Dung, L.T. and Chen, F., 2015. Late Permian to Early Triassic crustal evolution of the Kontum massif, central Vietnam: zircon U–Pb ages and geochemical and Nd–Hf isotopic composition of the Hai Van granitoid complex. International Geology Review, 1-12.
Honza, E., John, J. and Banda, R.M., 2000. An imbrication model for the Rajang accretionary complex in Sarawak, Borneo. Journal of Asian Earth Sciences 18, 751-759.
Hubert, J.F., 1962. A zircon-tourmaline-rutile maturity index and the interdependence of the composition of heavy mineral assemblages with the gross composition and texture of sandstones. Journal of Sedimentary Petrology 32, 440-450.
Hutchison, C.S., 1975. Ophiolites in southeast Asia. Geological Society of America Bulletin 86, 797-806.
Hutchison, C.S., 1977. Granite emplacement and tectonic subdivision of Peninsular Malaysia. Bull. Geol. Soc. Malaysia 9, 187-207.
Hutchison, C.S., 1989. Geological Evolution of South-East Asia. Oxford Monographs on Geology and Geophysics, 13. Clarendon Press, Oxford, 376 pp.
Hutchison, C.S., 1996. The 'Rajang Accretionary Prism' and 'Lupar Line' problem of Borneo. In: R. Hall and D.J. Blundell (Eds.), Tectonic Evolution of SE Asia. Geological Society London Special Publication 106, pp. 247-261.
Hutchison, C.S., 2005. Geology of North-West Borneo. Elsevier, Amsterdam, 421 pp.
Hutchison, C.S., 2010. Oroclines and paleomagnetism in Borneo and South-East Asia. Tectonophysics 496, 53-67.
Hutchison, C.S. and Tan, D.N.K., 2009. Geology of Peninsular Malaysia. The University of Malaya and the Geological Society of Malaysia, Kuala Lumpur, 479 pp.

1024 Ishihara, S. and Orihashi, Y., 2014. Zircon U-Pb age of the Triassic granitoids at Nui Phao, northern
1025 Viet Nam. Bulletin of the Geological Survey of Japan 65, 17-22.
1026 Jiang, X.-Y., Li, X.-H., Collins, W.J. and Huang, H.-Q., 2015. U-Pb age and Hf-O isotopes of detrital
1027 zircons from Hainan Island: Implications for Mesozoic subduction models. Lithos 239, 60-70.
1028 Johnsson, M.J., Stallard, R.F. and Meade, R.H., 1988. First-cycle quartz arenites in the Orinoco River
1029 basin, Venezuela and Colombia. The Journal of Geology 96, 263-277.
1030 Kirk, H.J.C., 1957. The Geology and Mineral Resources of the Upper Rajang and adjacent areas.
1031 British Territories Borneo Region Geological Survey, Memoir 8, 181 pp.
1032 Krähenbuhl, R., 1991. Magmatism, tin mineralization and tectonics of the Main Range, Malaysian
1033 Peninsula: Consequences for the plate tectonic model of Southeast Asia based on Rb-Sr, K-Ar
1034 and fission track data. Bulletin of the Geological Society of Malaysia 29, 1-100.
1035 Lan, C.-Y., Chung, S.-L., Lo, C.-H., Lee, T.-Y., Wang, P.-L., Li, H. and Van Toan, D., 2001. First evidence
1036 for Archean continental crust in northern Vietnam and its implications for crustal and
1037 tectonic evolution in Southeast Asia. Geology 29, 219-222.
1038 Lan, C.-Y., Chung, S.-L., Van Long, T., Lo, C.-H., Lee, T.-Y., Mertzman, S.A. and Jiun-San Shen, J., 2003.
1039 Geochemical and Sr–Nd isotopic constraints from the Kontum massif, central Vietnam on
1040 the crustal evolution of the Indochina block. Precambrian Research 122, 7-27.
1041 Liechti, P., Roe, F.W. and Haile, N.S., 1960. The Geology of Sarawak, Brunei and the western part of
1042 North Borneo. Geological Survey Department, British Territories of Borneo, Bulletin, 3, 360
1043 pp.
1044 Liu, J., Tran, M.-D., Tang, Y., Nguyen, Q.-L., Tran, T.-H., Wu, W., Chen, J., Zhang, Z. and Zhao, Z., 2012.
1045 Permo-Triassic granitoids in the northern part of the Truong Son belt, NW Vietnam:
1046 geochronology, geochemistry and tectonic implications. Gondwana Research 22, 628-644.
1047 Liu, R., Zhou, H., Zhang, L., Zhong, Z., Zeng, W., Xiang, H., Jin, S., Lu, X. and Li, C., 2009.
1048 Paleoproterozoic reworking of ancient crust in the Cathaysia Block, South China: Evidence
1049 from zircon trace elements, U-Pb and Lu-Hf isotopes. Chinese Science Bulletin 54, 1543-
1050 1554.
1051 Madon, M.B.H., 1999. Basin types, tectono-stratigraphic provinces and structural styles. The
1052 Petroleum Geology and Resources of Malaysia, 77-112.
1053 Mange, M.A. and Wright, D.T., 2007. Heavy minerals in use. Developments in Sedimentology 58.
1054 Elsevier, 1283 pp.
1055 Mao, J., Ye, H., Liu, K., Li, Z., Takahashi, Y., Zhao, X. and Kee, W.-S., 2013. The Indosinian collision–
1056 extension event between the South China Block and the Palaeo-Pacific plate: evidence from
1057 Indosinian alkaline granitic rocks in Dashuang, eastern Zhejiang, South China. Lithos 172, 81-
1058 97.
1059 Mat-Zin, I.C., 2000. Stratigraphic Position of Rangsi Conglomerate in Sarawak. Platform 1 (2), 25-31.
1060 McGilvery, T.A. and Cook, D.L., 2003. The influence of local gradients on accommodation space and
1061 linked depositional elements across a stepped slope profile, offshore Brunei, Shelf margin
1062 deltas and linked down slope petroleum systems: Global significance and future exploration
1063 potential: Gulf Coast Section SEPM 23rd Annual Research Conference. SEPM, pp. 387-419.
1064 Milroy, W.V., 1953. Geology of west Sarawak with notes on the palaeontology of west Sarawak by
1065 W.E. Crews. Sarawak Shell Oilfields ds Ltd. Report GR 602 (unpubl.).
1066 Morley, C.K., 2007a. Development of crestal normal faults associated with deepwater fold growth.
1067 Journal of Structural Geology 29, 1148-1163.
1068 Morley, C.K., 2007b. Interaction between critical wedge geometry and sediment supply in a deep-
1069 water fold belt. Geology 35, 139-142.
1070 Morley, C.K., 2009. Growth of folds in a deep-water setting. Geosphere 5, 59-89.
1071 Morley, C.K., 2012. Late Cretaceous–early Palaeogene tectonic development of SE Asia. Earth-
1072 Science Reviews 115, 37-75.
1073 Morton, A.C. and Hallsworth, C.R., 1994. Identifying provenance-specific features of detrital heavy
1074 mineral assemblages in sandstones. Sedimentary Geology 90, 241-256.

Moss, S.J., 1998. Embaluh Group turbidites in Kalimantan: evolution of a remnant oceanic basin in Borneo during the Late Cretaceous to Palaeogene. Journal- Geological Society London 155, 509-524.
Nemchin, A.A. and Cawood, P.A., 2005. Discordance of the U–Pb system in detrital zircons: implication for provenance studies of sedimentary rocks. Sedimentary Geology 182, 143-162.
Nguyen, T.T.B., Satir, M., Siebel, W. and Chen, F., 2004. Granitoids in the Dalat zone, southern Vietnam: age constraints on magmatism and regional geological implications. International Journal of Earth Sciences 93, 329-340.
Pearce, N.J.G., Perkins, W.T., Westgate, J.A., Gorton, M.P., Jackson, S.E., Neal, C.R. and Chenery, S.P., 1997. A Compilation of New and Published Major and Trace Element Data for NIST SRM 610 and NIST SRM 612 Glass Reference Materials. Geostandards Newsletter 21, 115-144.
Pettijohn, F.J., Potter, P.E. and Siever, R., 1987. Sand and Sandstone. Springer Science & Business Media, New York, 553 pp.
Pieters, P.E. and Sanyoto, P., 1993. Geology of the Pontianak/Nangataman Sheet area, Kalimantan. Map at 1:250000 scale. Geological Research and Development Centre, Bandung.
Pieters, P.E., Surono and Noya, Y., 1993. Geology of the Putussibau Sheet area, Kalimantan. Geological Survey of Indonesia, Directorate of Mineral Resources, Geological Research and Development Centre, Bandung, Quadrangle 1616, 1:250000.
Pieters, P.E., Trail, D.S. and Supriatna, S., 1987. Correlation of Early Tertiary rocks across Kalimantan. Indonesian Petroleum Association, Proceedings 16th annual convention Jakarta, 1987 I, 291-306.
Searle, M.P., Whitehouse, M.J., Robb, L.J., Ghani, A.A., Hutchison, C.S., Sone, M., Ng, S.W., Roselee, M.H., Chung, S.-L. and Oliver, G.J.H., 2012. Tectonic evolution of the Sibumasu-Indochina terrane collision zone in Thailand and Malaysia: constraints from new U-Pb zircon chronology of SE Asian tin granitoids. Journal of the Geological Society 169, 489.
Setiawan, N.I., Osanai, Y., Nakano, N., Adachi, T., Setiadji, L.D. and Wahyudiono, J., 2013. Late Triassic metatonalite from the Schwaner Mountains in West Kalimantan and its contribution to sedimentary provenance in the Sundaland. Berita Sedimentologi 12, 4-12.
Sevastjanova, I., 2007. Composition of Modern Detrital Sediments from the Malay Peninsula. MSc (unpublished) Thesis, Royal Holloway University of London, 155 pp.
Sevastjanova, I., Clements, B., Hall, R., Belousova, E.A., Griffin, W.L. and Pearson, N., 2011. Granitic magmatism, basement ages, and provenance indicators in the Malay Peninsula: Insights from detrital zircon U-Pb and Hf-isotope data. Gondwana Research 19, 1024-1039.
Sevastjanova, I., Hall, R. and Alderton, D., 2012. A detrital heavy mineral viewpoint on sediment provenance and tropical weathering in SE Asia. Sedimentary Geology 280, 179-194.
Shanmugam, G., 2016. Submarine fans: a critical retrospective (1950–2015). Journal of Palaeogeography 5, 110-184.
Shellnutt, J.G., Lan, C.-Y., Van Long, T., Usuki, T., Yang, H.-J., Mertzman, S.A., Iizuka, Y., Chung, S.-L., Wang, K.-L. and Hsu, W.-Y., 2013. Formation of Cretaceous Cordilleran and post-orogenic granites and their microgranular enclaves from the Dalat zone, southern Vietnam: Tectonic implications for the evolution of Southeast Asia. Lithos 182, 229-241.
Silva-Romo, G., Arellano-Gil, J., Mendoza-Rosales, C. and Nieto-Obregón, J., 2000. A submarine fan in the Mesa Central, Mexico. Journal of South American Earth Sciences 13, 429-442.
Sircombe, K.N., 2004. AgeDisplay: an EXCEL workbook to evaluate and display univariate geochronological data using binned frequency histograms and probability density distributions. Computers & Geosciences 30, 21-31.
Sláma, J. et al., 2008. Plešovice zircon — A new natural reference material for U–Pb and Hf isotopic microanalysis. Chemical Geology 249, 1-35.
Smyth, H.R., Hall, R. and Nichols, G.J., 2008. Significant volcanic contribution to some quartz-rich sandstones, East Java, Indonesia. Journal of Sedimentary Research 78, 335-356.

Smyth, H.R., Hamilton, P.J., Hall, R. and Kinny, P.D., 2007. The deep crust beneath island arcs: inherited zircons reveal a Gondwana continental fragment beneath East Java, Indonesia. Earth and Planetary Science Letters 258, 269-282.

Suttner, L.J., Basu, A. and Mack, G.H., 1981. Climate and the origin of quartz arenites. Journal of Sedimentary Research 51.

Tan, D.N.K., 1979. Lupar Valley, West Sarawak. Geological Survey of Malaysia, Report 13, 159 pp.

Tan, D.N.K., 1982. Lubok Antu Melange, Lupar Valley, West Sarawak: a Lower Tertiary subduction complex. Bulletin of the Geological Society of Malaysia 15, 31-46.

Tate, R.B., 1991. Cross-border correlation of geological formations in Sarawak and Kalimantan. Bulletin of the Geological Society of Malaysia 28, 63-96.

Tongkul, F., 1997. Sedimentation and tectonics of Paleogene sediments in central Sarawak. Bulletin of the Geological Society of Malaysia 40, 135-140.

Usuki, T., Lan, C.-Y., Wang, K.-L. and Chiu, H.-Y., 2013. Linking the Indochina block and Gondwana during the Early Paleozoic: Evidence from U–Pb ages and Hf isotopes of detrital zircons. Tectonophysics 586, 145-159.

van Bemmelen, R.W., 1949. The Geology of Indonesia. Government Printing Office, Nijhoff, The Hague, 732 pp.

van Hattum, M.W.A., 2005. Provenance of Cenozoic sedimentary rocks of northern Borneo. PhD Thesis, University of London, 467 pp.

van Hattum, M.W.A., Hall, R., Pickard, A.L. and Nichols, G.J., 2006. Southeast Asian sediments not from Asia: Provenance and geochronology of north Borneo sandstones. Geology 34, 589-592 551.

van Hattum, M.W.A., Hall, R., Pickard, A.L. and Nichols, G.J., 2013. Provenance and geochronology of Cenozoic sandstones of northern Borneo. Journal of Asian Earth Sciences 76, 266-282.

Vladimirov, A.G., Balykin, P.A., Anh, P.L., Kruk, N.N., Phuong, N.T., Travin, A.V., Hoa, T.T., Annikova, I.Y., Kuybida, M.L. and Borodina, E.V., 2012. The Khao Que-Tam Tao gabbro-granite massif, Northern Vietnam: A petrological indicator of the Emeishan plume. Russian Journal of Pacific Geology 6, 395-411.

Wang, S., Mo, Y., Wang, C. and Ye, P., 2016. Paleotethyan evolution of the Indochina Block as deduced from granites in northern Laos. Gondwana Research 38, 183-196.

Watkinson, I., Elders, C., Batt, G., Jourdan, F., Hall, R. and McNaughton, N.J., 2011. The timing of strike-slip shear along the Ranong and Khlong Marui faults, Thailand. Journal of Geophysical Research: Solid Earth 116.

Williams, H., Turner, F.J. and Gilbert, C.M., 1954. Petrography: An introduction to the study of rocks in thin section. W.H. Freeman, San Francisco, California, 406 pp.

Williams, P.R., Johnston, C.R., Almond, R.A. and Simamora, W.H., 1988. Late Cretaceous to Early Tertiary structural elements of West Kalimantan. Tectonophysics 148, 279-298.

Wolfenden, E.B., 1960. The Geology and Mineral Resources of the Lower Rajang Valley and adjoining areas, Sarawak. British Territories Borneo Region Geological Survey Department, Memoir 11, 167 pp.

Xu, C., Shi, H., Barnes, C.G. and Zhou, Z., 2016. Tracing a late Mesozoic magmatic arc along the Southeast Asian margin from the granitoids drilled from the northern South China Sea. International Geology Review 58, 71-94.

Yan, Q., Metcalfe, I. and Shi, X., 2017. U-Pb isotope geochronology and geochemistry of granites from Hainan Island (northern South China Sea margin): Constraints on late Paleozoic-Mesozoic tectonic evolution. Gondwana Research 49, 333-349.

Figure captions

Fig. 1: Geological map of Borneo modified after Hall and Breitfeld (2017), showing the extent of the Rajang Group in central Borneo. The research area in the Sibu Zone (Central Sarawak) is marked with the box.

Fig. 2: Geological map of Central Sarawak (Sibu Zone) modified after Liechti et al. (1960), Heng (1992) and Pieters et al. (1993) with locations of samples used in this study. Bold samples have detrital zircon U-Pb ages.

Fig. 3: Field photographs of the Lupar Formation and Layar Member. A – Alternations of fine to medium grained sandstone beds with thin layers of mudstone of the Lupar Formation (STB104). Inset figure: Close-up of the alternations. B – Slumping within alternations of sandstone and shale of the Lupar Formation (STB104). C – Alternations of slumped thick sandstone with shale and siltstone in the Layar Member (TB179). D – Close-up of the slump folds (TB179). E – Conglomerate bed composed of mud clasts within white amalgamated sandstone in the Layar Member (TB182). F – Close-up of the mudflake conglomerate in the Layar Member (TB182). G – Horizontal to rippled sandstone with thin mud layers in the Layar Member (TB182). H – Turbidite composed of Bouma A (graded sandstone) and B (horizontal laminated sandstone) above E (mudstone) in the Layar Member (TB183). I – Slate in the Layar Member (STB117).

Fig. 4: Field photographs of the Kapit Member. A – Thick sandstone succession on top of mudstone-siltstone alternations at Bukit Sebangkoi in the lower Kapit Member (TB42). B – Sharp contact of thick sandstone succession with mudstone-siltstone alternations (TB42). C – Massive slumping in sandstone-siltstone-shale alternations in the upper Kapit Member (TB43). D – Load structures at the base of vertical meta-sandstone bed in the upper Kapit Member (TB238). E – Upright tight antiform in meta-sandstone beds of the upper Kapit Member (TB235).

Fig. 5: Field photographs of the Pelagus Member. A – Alternation of sandstone and shale overlain by thick amalgamated sandstone with irregular base (TB44). B – Close-up of the irregular contact. C – Close-up of the thinly bedded sandstone-mudstone alternations. D – Ripple marks on the bedding plane at the top of a sandstone bed (TB191). E – Bioturbation in sandstone bed (TB193). F – Horizontal and ripple lamination (climbing ripples) in sandstone bed (TB191). G – Load casts at the base of sandstone bed (TB248). H – Thick amalgamated sandstone packages interbedded with mudstone at the Bukit Tanggi quarry (TB191).

Fig. 6: Field photographs of the Pelagus, Metah and Bawang Members. A – Bioturbation and convolute bedding with in sandstone-mudstone alternations (heterolithics) of the Pelagus Member (TB193). B – Soft-sediment deformation within the Pelagus Member, resulting in polygonal normal

faults within a sandstone bed (TB193). C – Mudflake conglomerate in the Pelagus Member composed of elongated mud clasts (TB193). D – Soft-sediment deformation in the Pelagus Member with irregular mudstone-sandstone alternations displaced along syn-sedimentary faults (TB193). E-Upright isoclinal fold within the Metah Member (TB196). F – Slumped alternations of thin shale and siltstone within the Metah Member (TB202). G – Amalgamated sandstone packages between thick shale and siltstone alternations in the Metah Member (TB203). Inset figure shows the erosive basal contact of the sandstone. H – Thick sandstone bed between thick siltstone-mudstone alternations (TB47). Inset figure shows the sharp to slight irregular contact of the thick sandstone with the siltstone-mudstone alternations. I – Moderately dipping shale-siltstone alternations of the Bawang Member unconformably overlain by the Tunggal-Rangsi Conglomerate (TB199). Inset figure shows a close-up of the shale-siltstone alternations of the Bawang Member.

Fig. 7: QFL and QmFLt plots of framework detrital modes showing composition of Rajang Group sandstones. QFL diagram for classification for arkosic rocks (0-15% matrix) and for wackes (15-75% matrix) after Pettijohn et al. (1987). QFL and QmFLt diagram for provenance after Dickinson et al. (1983).

Fig. 8: Photomicrographs of selected heavy minerals from the Rajang Group in plane polarised light.

Fig. 9: Backscattered SEM images. Scale bar is 50 micron. A – Selected heavy mineral grains of the Rajang Group samples. B – Different zircon types from the Rajang Group samples.

Fig. 10: Heavy mineral abundances in the Rajang Group sandstones. A – Variations shown as 100% vertical stacked area plots. B – ZTR (zircon-tourmaline-rutile) heavy mineral index and ZTi (zircon-tourmaline) ratio, showing significant variations that are interpreted as different provenance indicators.

Fig. 11: U-Pb detrital zircon age histograms with probability density plot for samples of Lupar Formation, Layar Member and lower Kapit Member (Unit 1), which have Cretaceous, Permian-Triassic and Precambrian zircon populations. Histograms for each sample use a bin size of 10 Ma for Phanerozoic ages and 50 Ma for Precambrian ages.

Fig. 12: U-Pb detrital zircon age histograms with probability density plot for samples of upper Kapit and Pelagus Member (Unit 2), showing major Cretaceous population. Histograms for each sample use a bin size of 10 Ma for Phanerozoic ages and 50 Ma for Precambrian ages.

Fig. 13: U-Pb detrital zircon age histograms with probability density plot for samples of the Metah (Unit 3) and Bawang Member. Metah Member samples have Cretaceous, Permian-Triassic and Silurian and Precambrian populations. Bawang Member samples have abundant Cretaceous and

Jurassic ages. Sample TB47 has also abundant Triassic ages. Histograms for each sample use a bin size of 10 Ma for Phanerozoic ages and 50 Ma for Precambrian ages.

Fig. 14: SRTM image of Central Sarawak (Sibu Zone) showing major lineaments and the newly proposed subdivision for the Rajang Group.

Fig. 15: Reconstruction of deposition and provenance of the Rajang Group in the Late Cretaceous to ?Late Eocene based on Smyth et al. (2007), Hall (2012), Hennig et al. (2016, 2017), Breitfeld et al. (2017) and this study. Rajang Unit 1 was sourced in the Late Cretaceous (Maastrichtian) to Early Eocene by the Schwaner Mountains, and West Borneo and the Malay Tin Belt. Rajang Unit 2 was predominantly sourced by the Schwaner Mountains in the Early to Middle Eocene. Rajang Unit 3 was sourced by the Schwaner Mountains, and West Borneo and the Malay Tin Belt in the Middle to ?Late Eocene. Note: The Bawang Member provenance is similar to Unit 2 or the base of Unit 1. It could indicate deposition in the Middle Eocene or in the Late Cretaceous. A Late Eocene age for this member is unlikely. Faults in Thailand (MPF, TPF, RF, KMF) after Watkinson et al. (2011), Morley (2012) and Fyhn et al. (2016). Khorat Basin/Plateau and equivalents in the Thai-Malay Peninsula after Clements et al. (2011) and Fyhn et al. (2016).

Table captions

Table 1: Light mineral modes for the Rajang Group samples in the Sibu Zone, Central Sarawak. (Qm = monocrystalline quartz, Qmu = monocrystalline undulary quartz, Qv = volcanic quartz, Qp = polycrystalline quartz, Ch = chert, Fp = plagioclase, Fk = K-feldspar, Lm = metamorphic lithic fragments, Ls = sedimentary lithic fragments, Lv = volcanic lithic fragments, H = heavy mineral, Mt = matrix, Lithics (L) = Lm+Ls+Lv, Total lithics (Lt) = Lm+Ls+Lv+Qp+Ch, Total Qm = Qm+Qmu+Qv). (*considered to be Pelagus Member, but the location is in an area mapped by Heng (1992) as Metah Member)

Table 2.1: Total heavy mineral counts of the Rajang Group samples in the Sibu Zone, Central Sarawak.

Table 2.2: Heavy mineral percentages of the Rajang Group samples in the Sibu Zone, Central Sarawak.

Table 3: Commonly used heavy mineral ratios and counts of heavy minerals for index calculation after Hubert (1962); Morton and Hallsworth (1994) and Mange and Wright (2007).

Table 4: Summary of the new three-fold subdivision of the Rajang Group. Age incorporates zircon data of this study and previous paleontology published in Liechti et al. (1960) and Hutchison (2005).

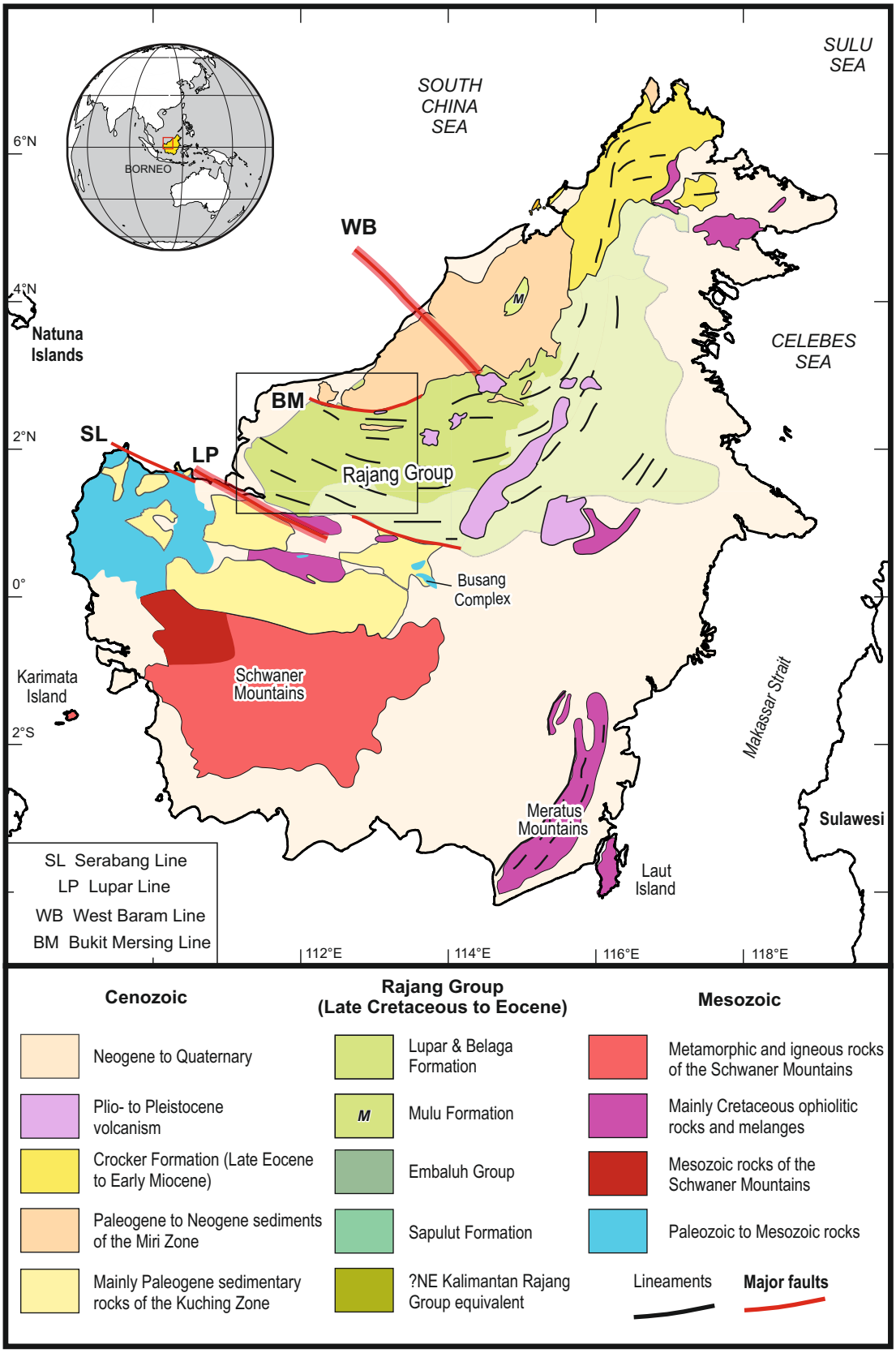
SULU SEA
SOUTH CHINA SEA
BORNEO
6°N
4°N
2°N
0°
2°S
WB
BM
SL
LP
Natuna Islands
CELEBES SEA
Rajang Group
Busang Complex
Schwaner Mountains
Karimata Island
Makassar Strait
Meratus Mountains
Sulawesi
Laut Island
SL Serabang Line
LP Lupar Line
WB West Baram Line
BM Bukit Mersing Line
112°E
114°E
116°E
118°E
Cenozoic
Neogene to Quaternary
Plio- to Pleistocene volcanism
Crocker Formation (Late Eocene to Early Miocene)
Paleogene to Neogene sediments of the Miri Zone
Mainly Paleogene sedimentary rocks of the Kuching Zone
Rajang Group (Late Cretaceous to Eocene)
Lupar & Belaga Formation
M
Mulu Formation
Embaluh Group
Sapulut Formation
?NE Kalimantan Rajang Group equivalent
Mesozoic
Metamorphic and igneous rocks of the Schwaner Mountains
Mainly Cretaceous ophiolitic rocks and melanges
Mesozoic rocks of the Schwaner Mountains
Paleozoic to Mesozoic rocks
Lineaments
Major faults

Fig.1

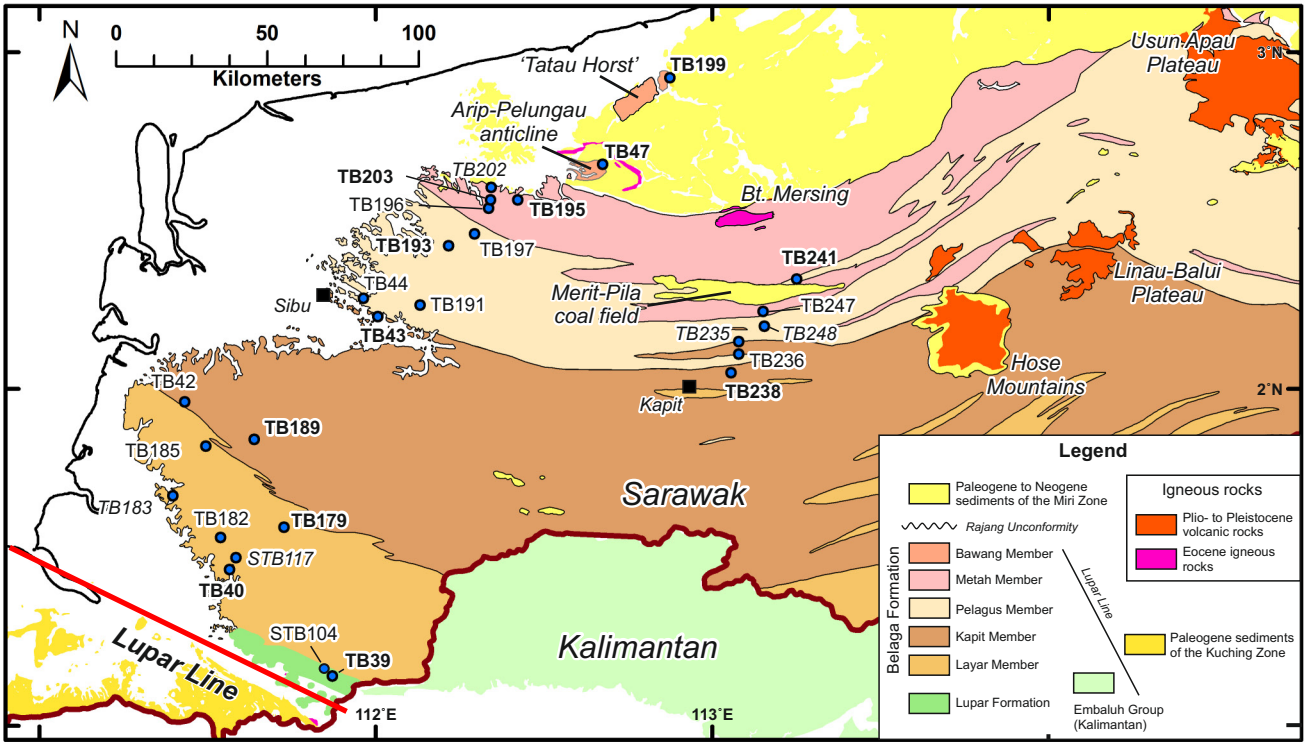
N
0
50
100
Kilometers
'Tatau Horst'
TB199
Usun Apau Plateau
3°N
Arip-Pelungau anticline
TB47
TB203
TB202
TB196
TB195
Bt. Mersing
TB193
TB197
TB241
Linau-Balui Plateau
TB44
Sibu
TB191
Merit-Pila coal field
TB247
TB43
TB235
TB248
TB236
TB42
Hose Mountains
TB238
Kapit
2°N
TB189
TB185
Sarawak
TB183
TB182
TB179
STB117
TB40
STB104
Kalimantan
Lupar Line
TB39
112°E
113°E
Legend
Paleogene to Neogene sediments of the Miri Zone
Rajang Unconformity
Belaga Formation
Bawang Member
Metah Member
Pelagus Member
Kapit Member
Layar Member
Lupar Formation
Lupar Line
Embaluh Group (Kalimantan)
Igneous rocks
Plio- to Pleistocene volcanic rocks
Eocene igneous rocks
Paleogene sediments of the Kuching Zone

Fig.2

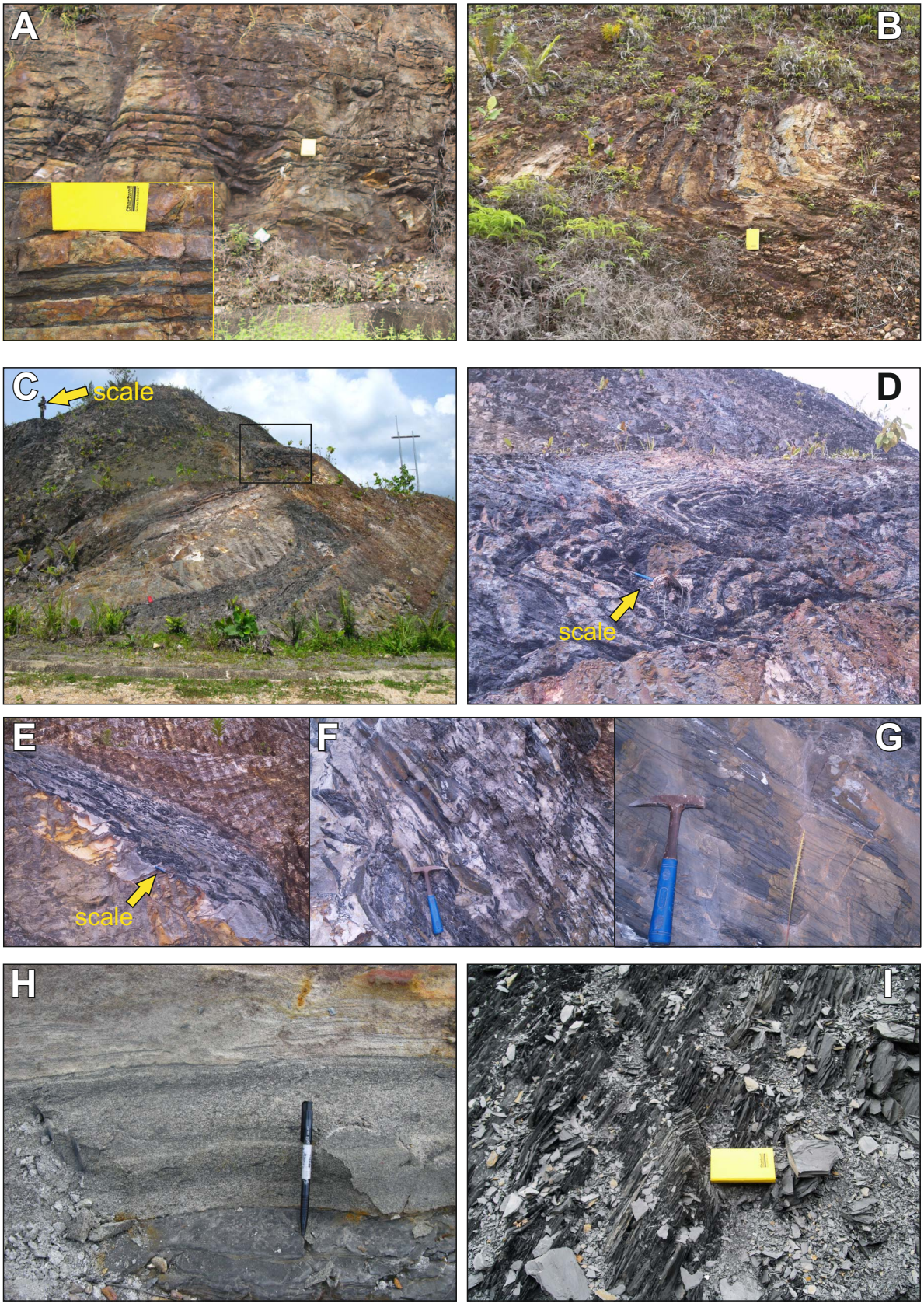

Fig.3

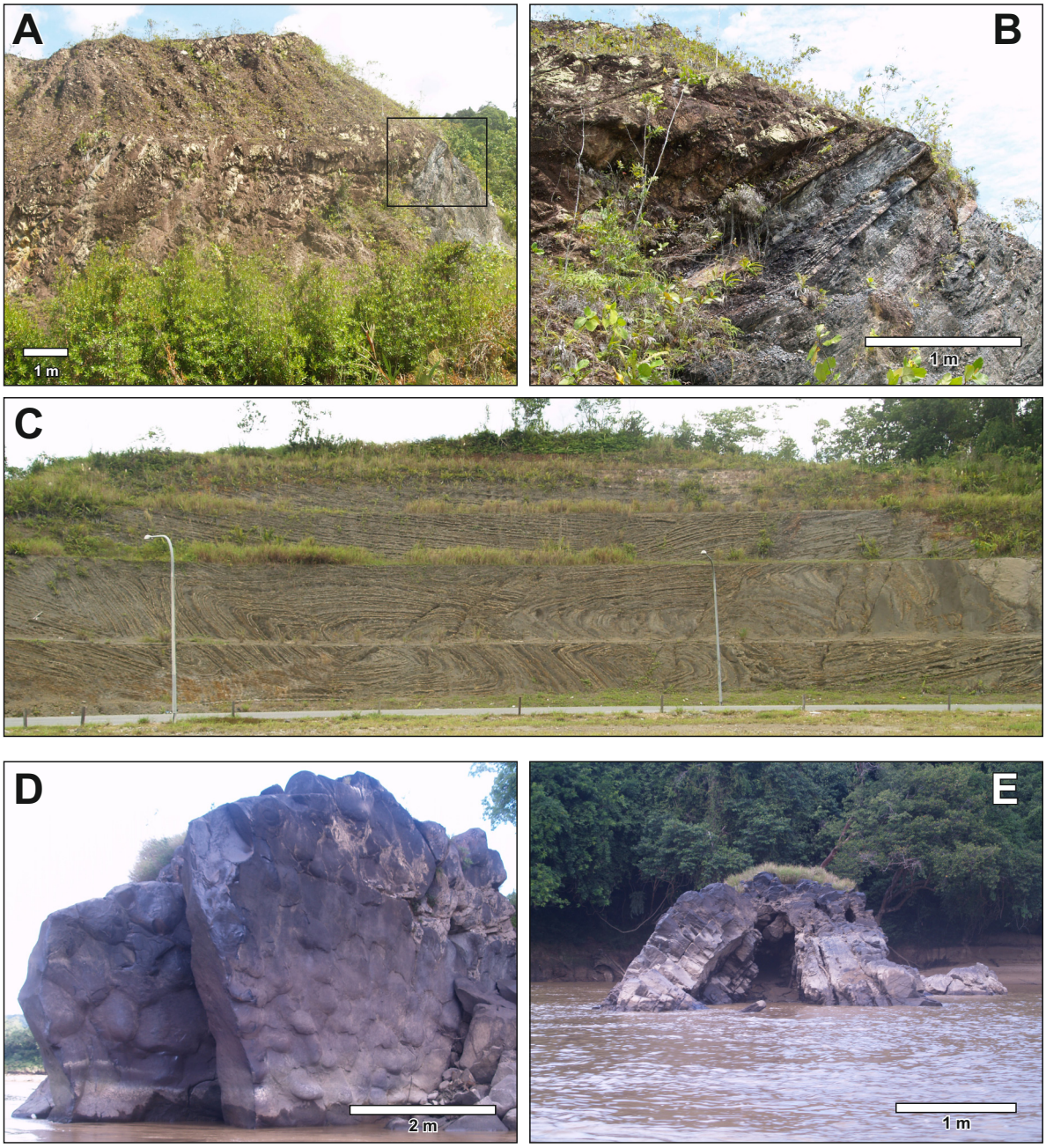

Fig.4

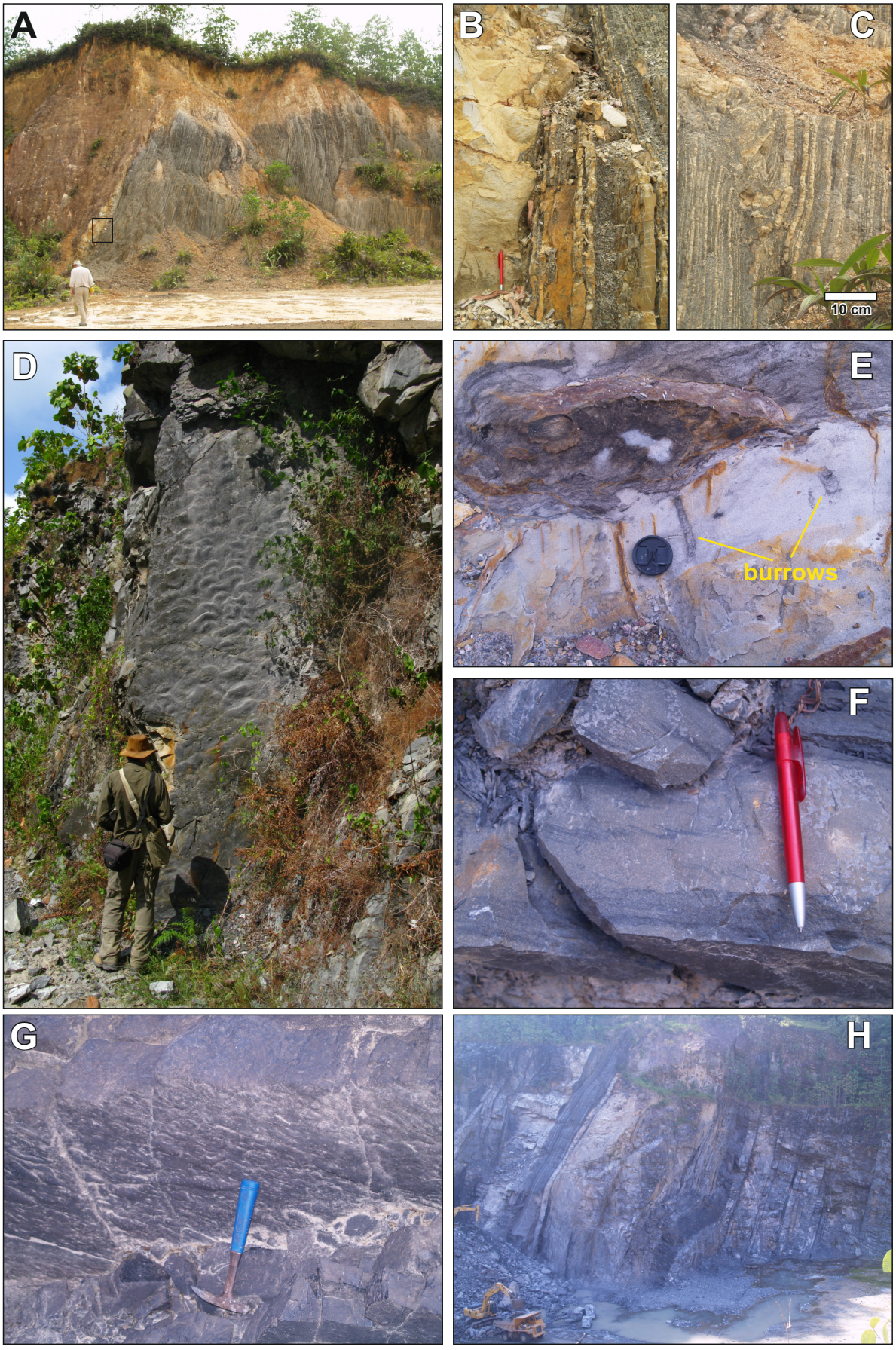

Fig.5

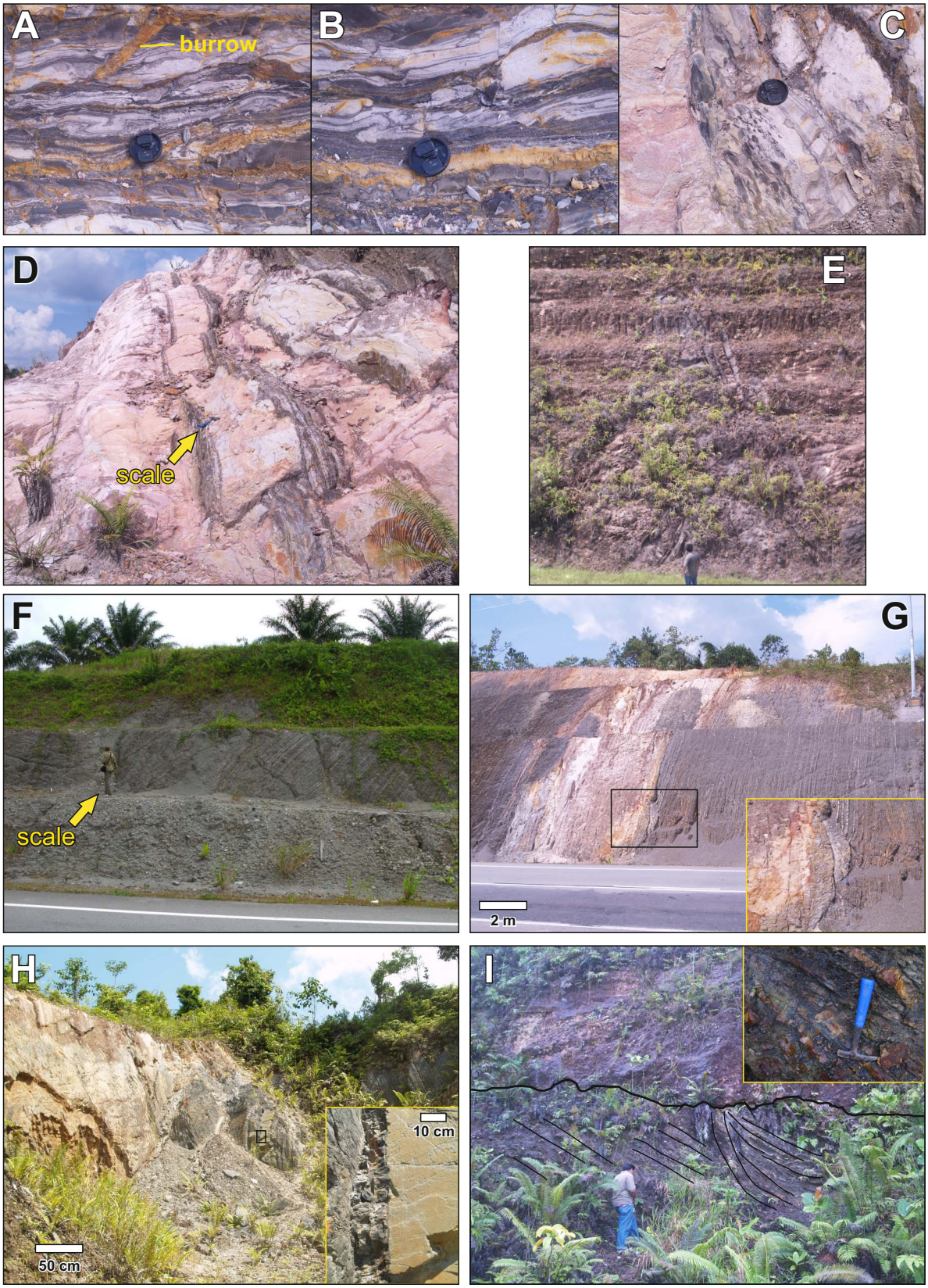

Fig.6

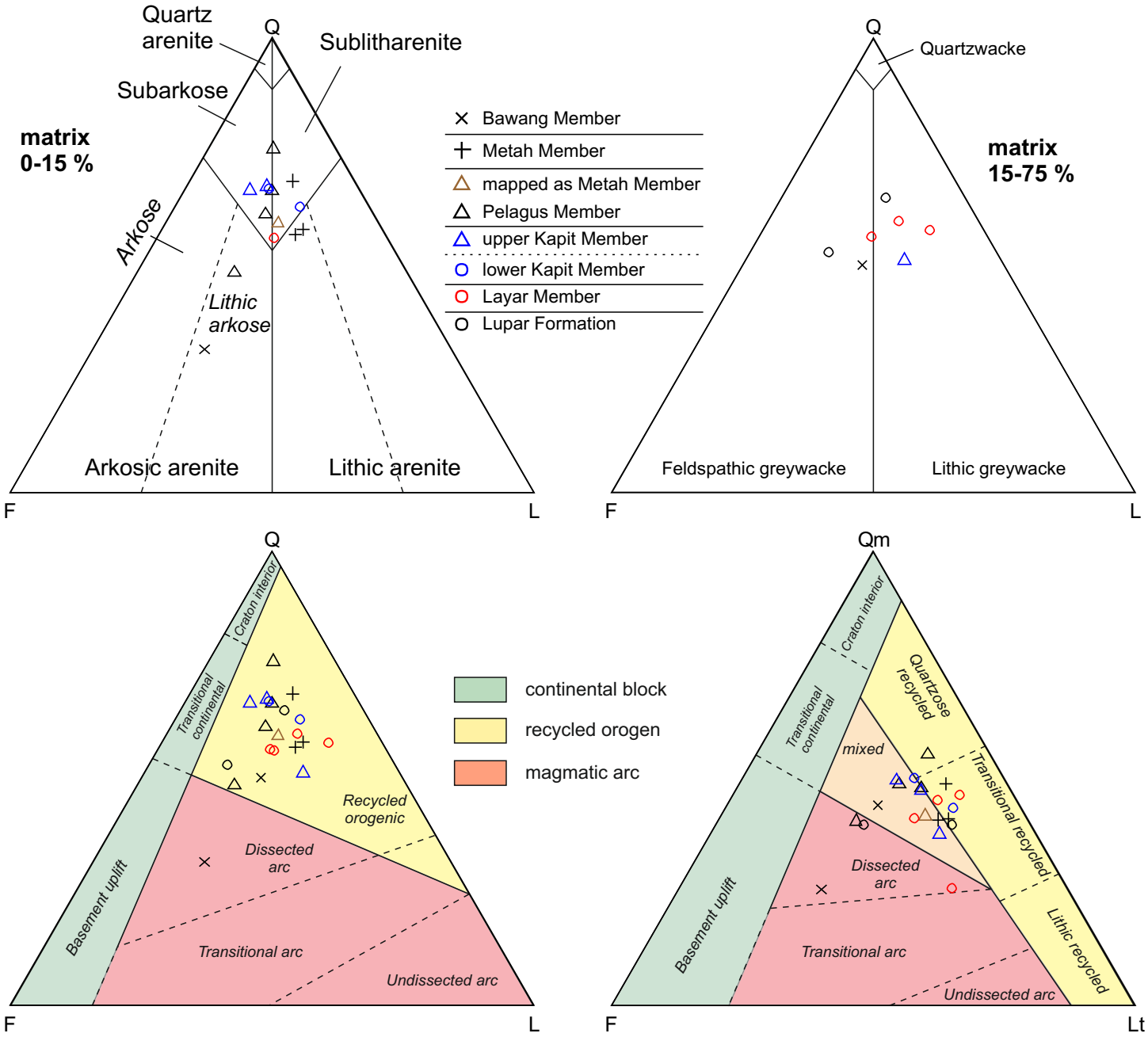
Quartz arenite
Q
Sublitharenite
Subarkose
matrix 0-15 %
Arkose
Lithic arkose
Arkosic arenite
Lithic arenite
F
L
Bawang Member
Metah Member
mapped as Metah Member
Pelagus Member
upper Kapit Member
lower Kapit Member
Layar Member
Lupar Formation
Q
Quartzwacke
matrix 15-75 %
Feldspathic greywacke
Lithic greywacke
F
L
Q
Craton interior
Transitional continental
Recycled orogenic
Basement uplift
Dissected arc
Transitional arc
Undissected arc
F
L
continental block
recycled orogen
magmatic arc
Qm
Craton interior
Quartzose recycled
Transitional continental
mixed
Transitional recycled
Basement uplift
Dissected arc
Lithic recycled
Transitional arc
Undissected arc
F
Lt

Fig.7

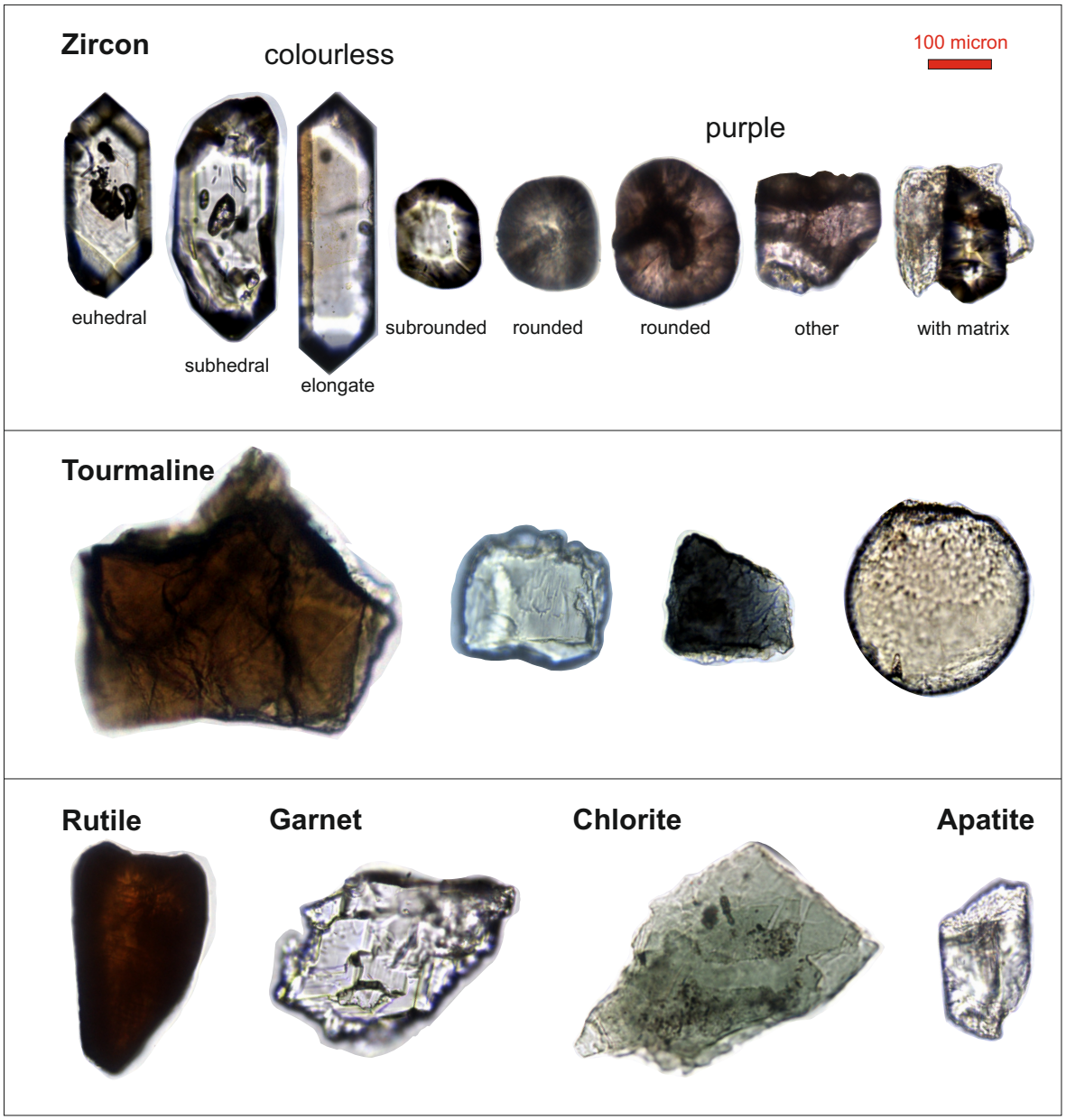
Zircon
colourless
100 micron
purple
euhedral
subhedral
elongate
subrounded
rounded
rounded
other
with matrix
Tourmaline
Rutile
Garnet
Chlorite
Apatite

Fig.8

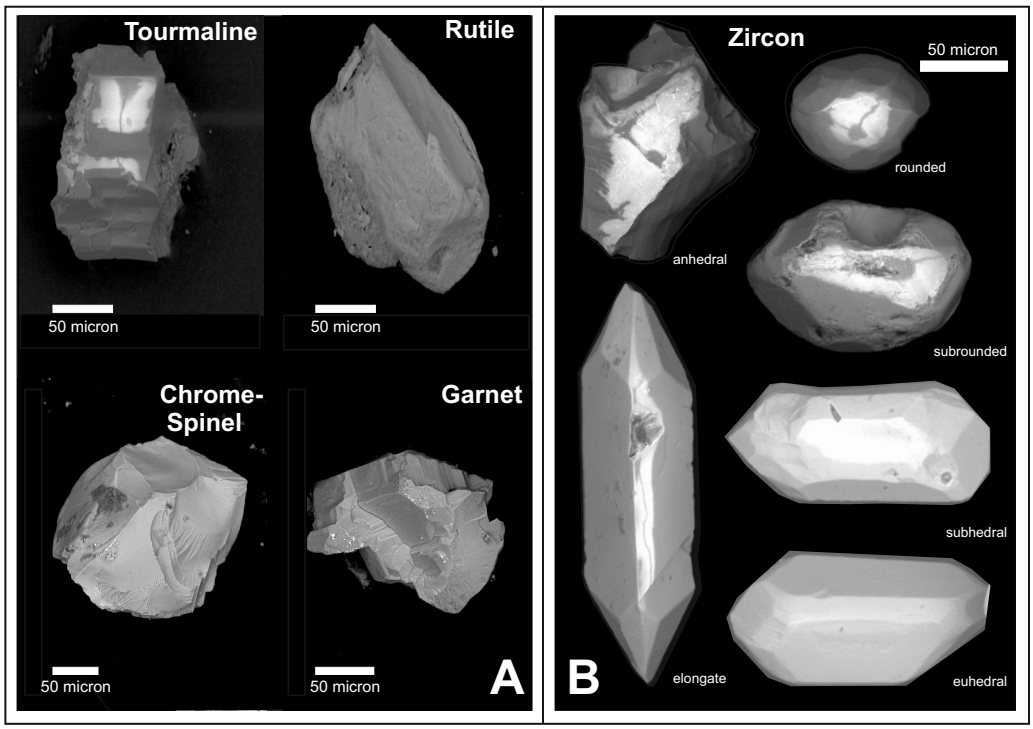
Tourmaline
50 micron
Rutile
50 micron
Chrome-
Spinel
50 micron
Garnet
50 micron
A
Zircon
50 micron
rounded
anhedral
subrounded
subhedral
elongate
euhedral
B

Fig.9

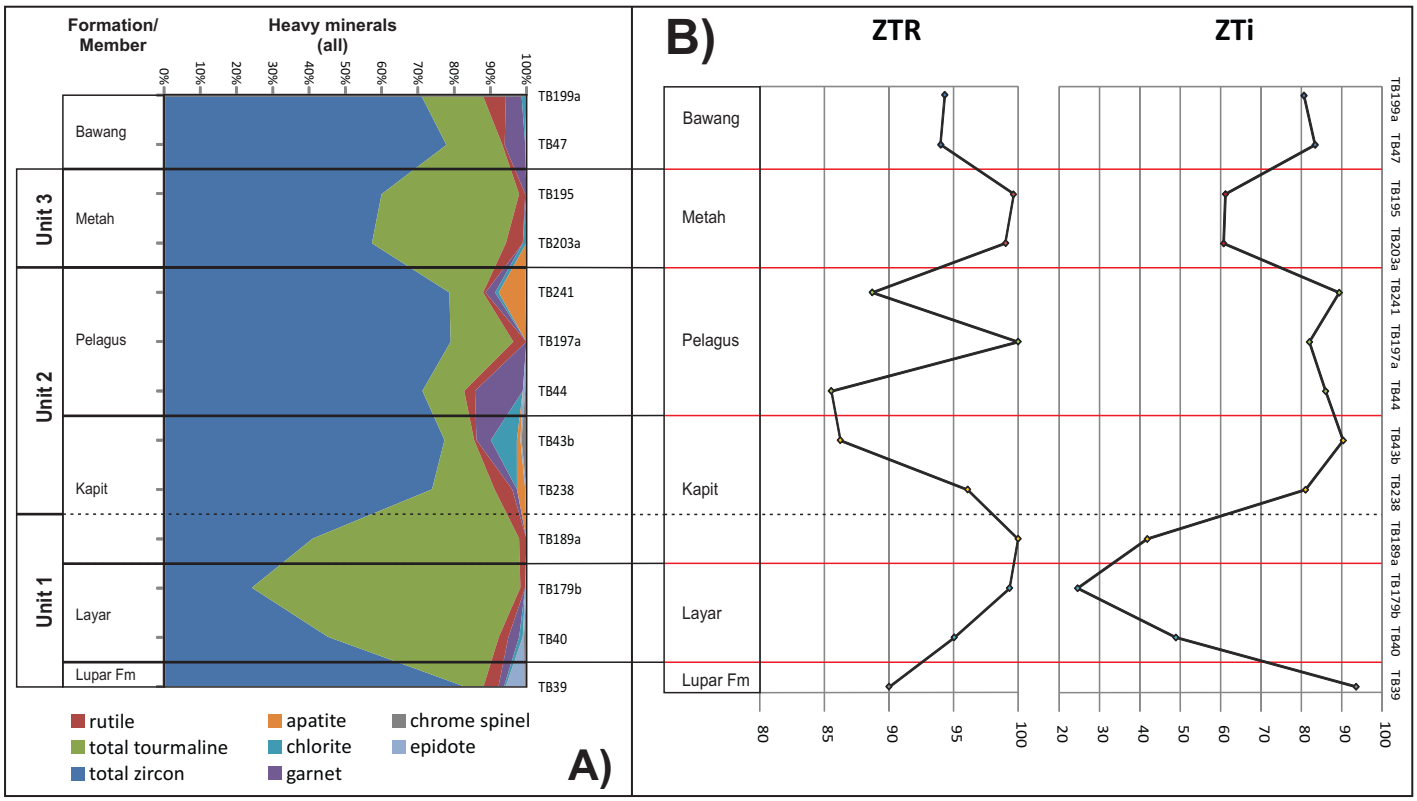
Formation/ Member
Heavy minerals (all)
0%
10%
20%
30%
40%
50%
60%
70%
80%
90%
100%
Unit 3
Unit 2
Unit 1
Bawang
Metah
Pelagus
Kapit
Layar
Lupar Fm
TB199a
TB47
TB195
TB203a
TB241
TB197a
TB44
TB43b
TB238
TB189a
TB179b
TB40
TB39
rutile
total tourmaline
total zircon
apatite
chlorite
garnet
chrome spinel
epidote
A)
B)
ZTR
ZTi
80
85
90
95
100
20
30
40
50
60
70
80
90
100

Fig.10

Lupar Formation, Layar and lower Kapit Member (Unit 1)

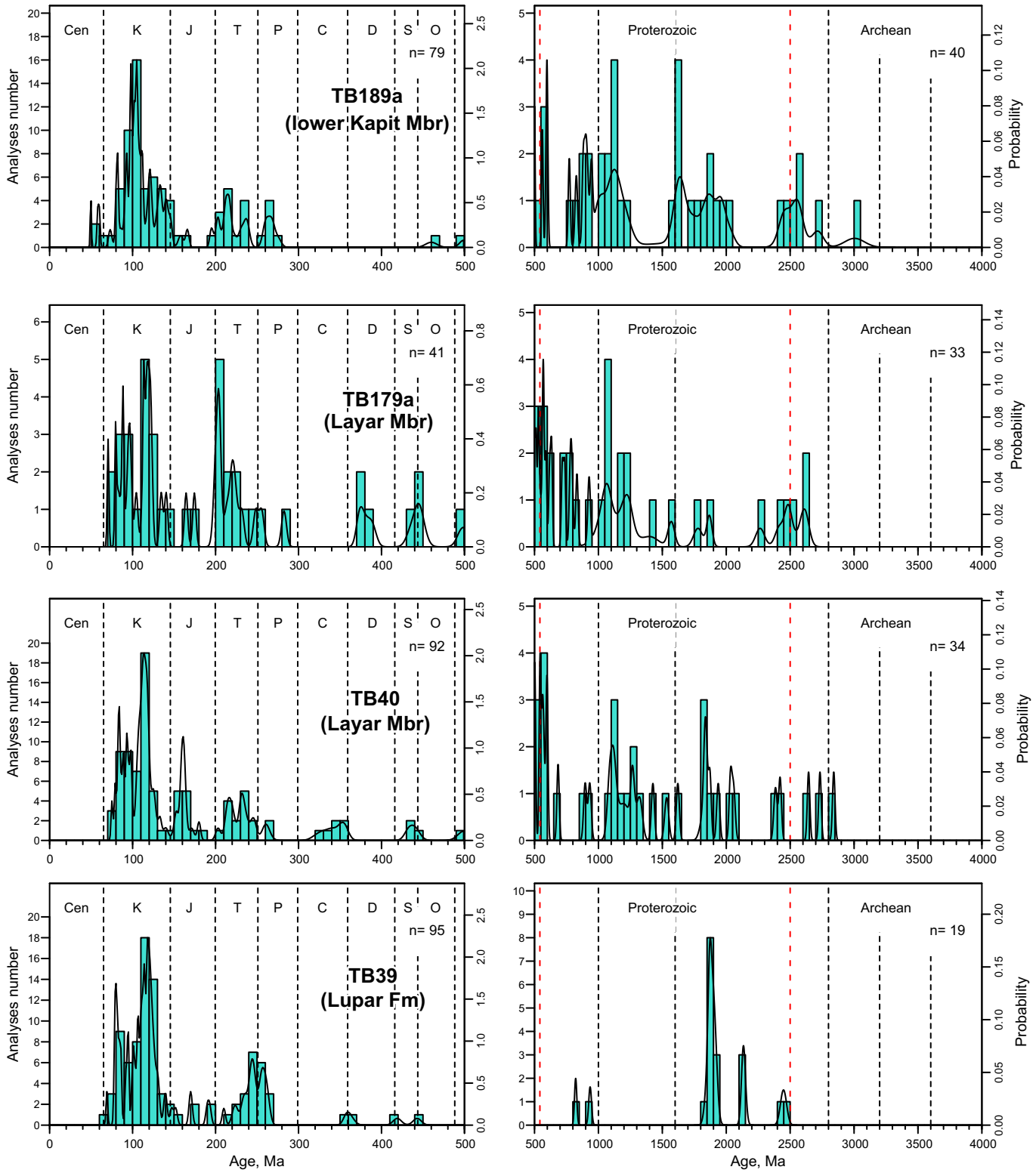

Fig.11

Upper Kapit and Pelagus Member (Unit 2)

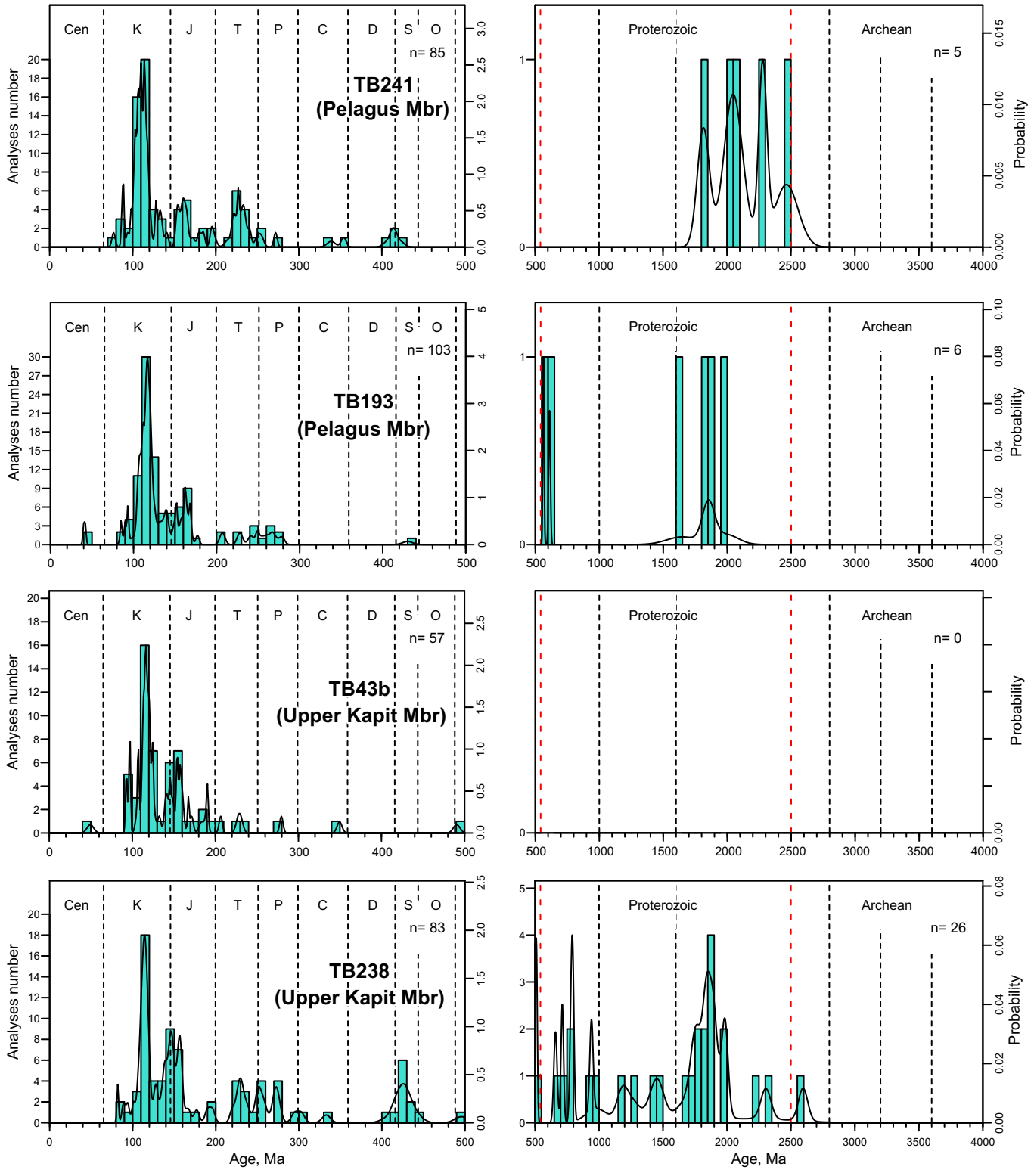

Fig.12

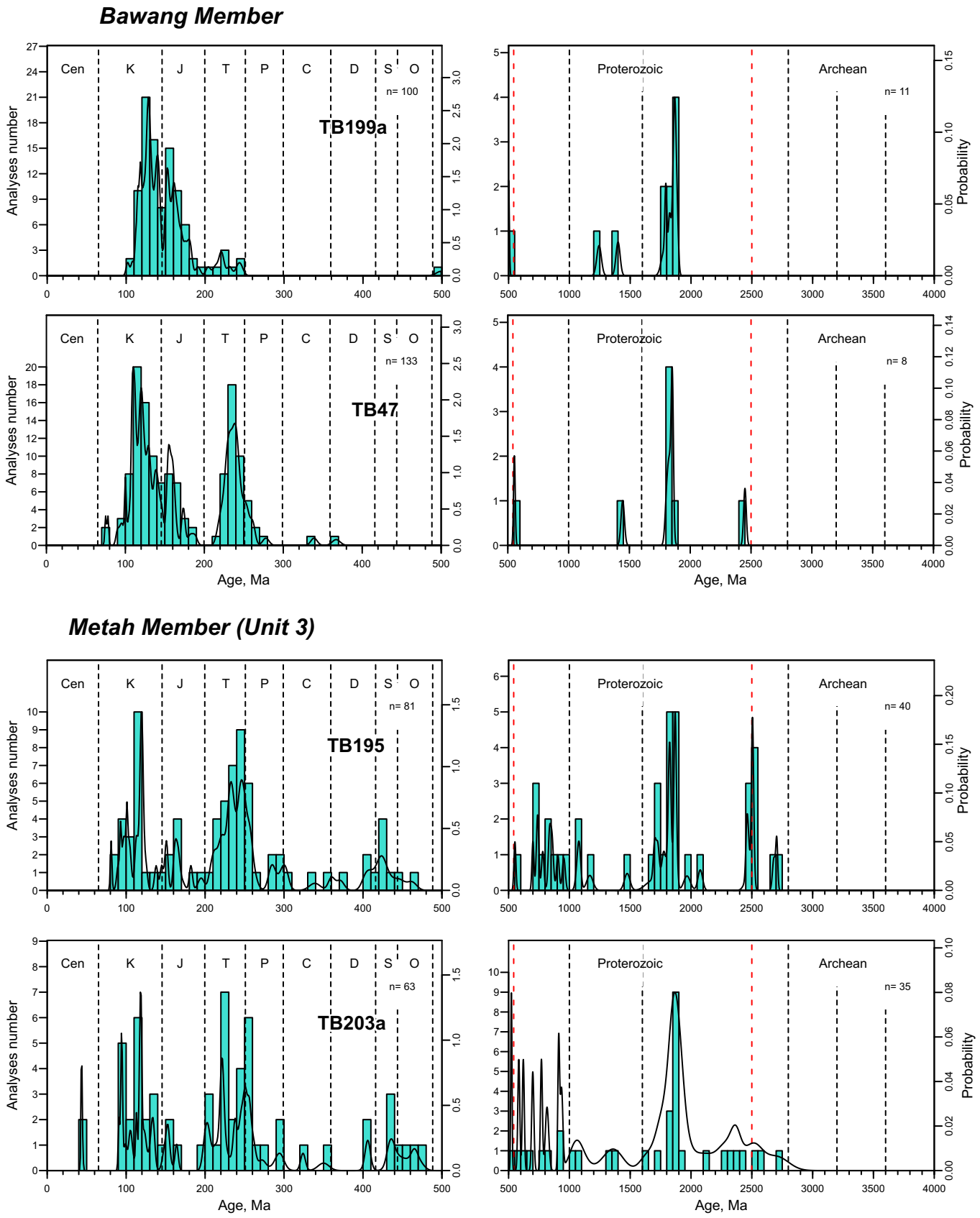
Bawang Member
Cen
K
J
T
P
C
D
S
O
n= 100
TB199a
Proterozoic
Archean
n= 11
Analyses number
Probability
n= 133
TB47
n= 8
Age, Ma
Metah Member (Unit 3)
n= 81
TB195
n= 40
n= 63
TB203a
n= 35

Fig.13

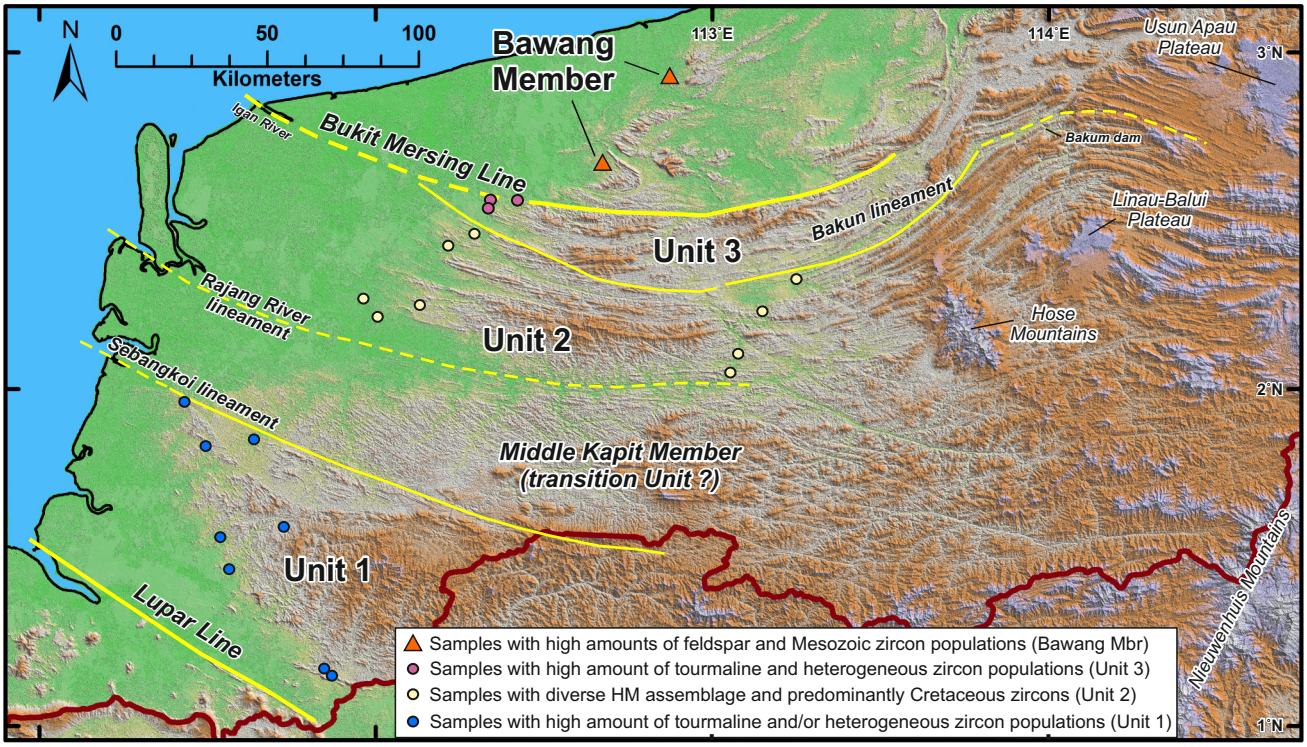
N
0
50
100
Kilometers
Bawang Member
113˚E
114˚E
Usun Apau Plateau
3˚N
Igan River
Bukit Mersing Line
Bakum dam
Bakun lineament
Linau-Balui Plateau
Unit 3
Rajang River lineament
Unit 2
Hose Mountains
Sebangkoi lineament
2˚N
Middle Kapit Member (transition Unit ?)
Unit 1
Lupar Line
Nieuwenhuis Mountains
Samples with high amounts of feldspar and Mesozoic zircon populations (Bawang Mbr)
Samples with high amount of tourmaline and heterogeneous zircon populations (Unit 3)
Samples with diverse HM assemblage and predominantly Cretaceous zircons (Unit 2)
Samples with high amount of tourmaline and/or heterogeneous zircon populations (Unit 1)
1˚N

Fig.14

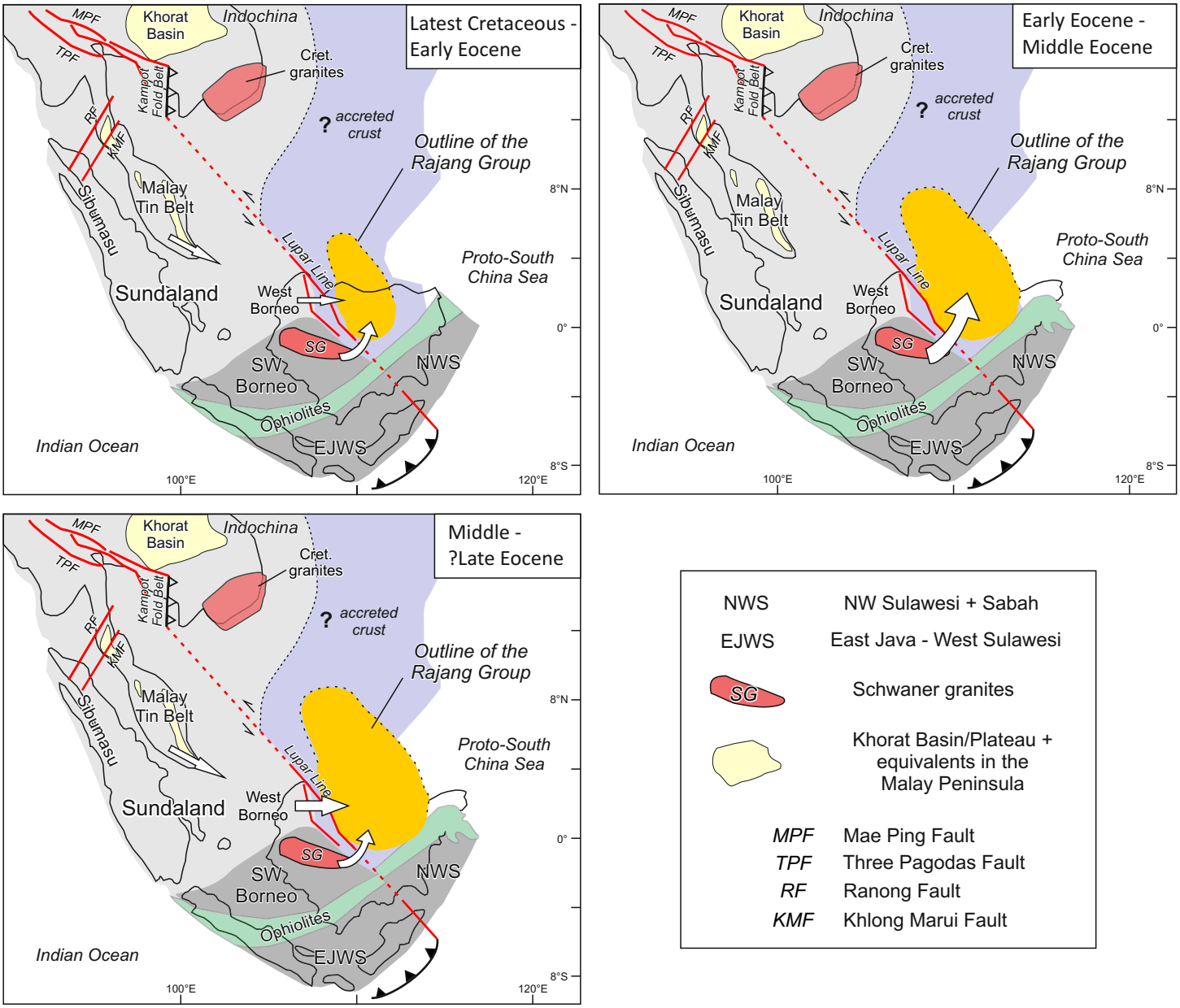
Latest Cretaceous - Early Eocene
Early Eocene - Middle Eocene
Middle - ?Late Eocene
MPF
TPF
RF
KMF
Khorat Basin
Indochina
Kampot Fold Belt
Cret. granites
? accreted crust
Outline of the Rajang Group
Proto-South China Sea
Malay Tin Belt
Sibumasu
Sundaland
West Borneo
Lupar Line
SG
SW Borneo
NWS
Ophiolites
EJWS
Indian Ocean
8°N
0°
8°S
100°E
120°E
NWS NW Sulawesi + Sabah
EJWS East Java - West Sulawesi
SG Schwaner granites
Khorat Basin/Plateau + equivalents in the Malay Peninsula
MPF Mae Ping Fault
TPF Three Pagodas Fault
RF Ranong Fault
KMF Khlong Marui Fault

Fig.15